https://doi.org/10.5194/cp-2021-96
Preprint. Discussion started: 24 August 2021

Climate of the Past Discussions

Multiple Proxy Estimates of pCO_2 in the Hauterivian–Barremian of the Laiyang Basin, Eastern China

Peihong Jin[1,2], Mingzheng Zhang[1,*] , Xiangtong Lei[3], Baoxia Du[2,4], Junling Dong[5], Bainian Sun[2,3]

[1] *Key Laboratory of Petroleum Resources, Northwest Institute of Eco-Environment and Resources, Chinese Academy of Sciences, Gansu Province, Lanzhou 730000, China*

[2] *State Key Laboratory of Paleobiology and Stratigraphy, Nanjing Institute of Geology and Paleontology, CAS, Nanjing 210008, China*

[3]*Yunnan Key Laboratory for Palaeobiology, Institute of Palaeontology, Yunnan University, Yunnan Province, Kunming 650000, China*

[4]*School of Earth Science, Lanzhou University and Key Laboratory of Mineral Resources in Western China (Gansu Province), Lanzhou 730000, China*

[5]*State Key Laboratory of Oil and Gas Reservoir Geology and Exploitation, Institute of Sedimentary Geology, Chengdu University of Technology, Chengdu 610059, China*

* Corresponding author.

E–mail address: zhangmzh08@lzb.ac.cn (M. Z. Zhang)

https://doi.org/10.5194/cp-2021-96
Preprint. Discussion started: 24 August 2021

Climate of the Past Discussions

Abstract: In recent decades, several proxies have been developed to reconstruct atmospheric paleo-CO_2 concentrations (pCO_2). The confidence in paleo-CO_2 estimates can be increased by comparing results from multiple proxies with multiple species at a single site. Here we present a new pCO_2 record for the Hauterivian–Barremian using three methods based on two fossil coniferous species (*Cupressinocladus* sp. and *Brachyphyllum obtusum*) collected from Laiyang Basin, eastern China. The pCO_2 values were approximately 579–663 ppmv (recent standardization) and 966–1106 ppmv (carboniferous standardization) based on the stomatal ratio (*SR*)-based method, and about 472–525 ppmv based on the mechanistic model. Both of these two methods were highly coincident with other *SR*-based and geochemical reconstructions for the early stage of the Early Cretaceous. The pCO_2 value estimated using the carbon isotopes model was approximately 472–525 ppmv, which is generally lower than the pCO_2 valueestimated using the other methods. The mechanistic model may be widely applied to more fossil taxa than the *SR*-based method and retains sensitivity at high pCO_2. Furthermore, by comparing with other pCO_2 records and Weissert event in the Early Cretaceous, the pCO_2 values obtained from this study indicate a relatively low atmospheric CO_2 concentration during the Hauterivian–Barremian, and reflect the cooling event in the last stage of the Weissert event.

Keywords: Hauterivian–Barremian, Cuticle, Stomatal ratio, Mechanistic model, Carbon isotope model, Weissert event

1. Introduction

The Early Cretaceous was a critical period for the globe to enter a typical greenhouse climate period in geological history. During this period, major changes occurred in the marine and terrestrial environment, a large number of rift basins were formed, large igneous provinces and oceanic anoxic event (OAE) frequently occurred, and the global climate fluctuated between arid and humid climates (Skelton et al., 2003; Föllmi, 2012; Jenkyns, 2010). These events have greatly affected the development and evolution of marine and terrestrial organisms (Skelton et al., 2003; Föllmi, 2012; Jenkyns, 2010).

Atmospheric CO_2 is one of the most important greenhouse gases and it is considered to be a major factor in global warming (Boucot and Gray, 2001; Royer, 2006; Fletcher et al., 2008; Wang

https://doi.org/10.5194/cp-2021-96
Preprint. Discussion started: 24 August 2021


Climate of the Past Discussions

et al., 2014). Fluctuations in atmospheric CO_2 concentrations have a significant impact on the carbonate saturation state in the oceans and the weathering rate of the continental surface, further leading to the mass extinctions of marine and terrestrial species (Li et al., 2019). As a result, a more complete understanding of atmospheric paleo-CO_2 concentration (pCO_2) variations during the Early Cretaceous could potentially provide us with a good reference for reconstructing the past climate environment and predicting the response of climate to future elevated atmospheric CO_2 levels.

In addition to early long–term atmospheric carbon cycle models (such as GEOCARB, GEOCARB II, GEOCARB III, GEOCARBSULF and COPSE), several proxies have been developed to reconstruct pCO_2 in recent decades, including stable carbon isotopes of paleosols, boron isotope pH derived from marine carbonate microfossils and marine alkenones, stable carbon isotopes of fossil liverworts, and stomatal parameters from terrestrial vascular plant fossils (Mcelwain and Chaloner, 1995; Pearson and Palmer, 2000; Beerling et al., 2001; Beerling and Royer, 2002a, 2002b; Retallack, 2005; Fletcher et al., 2005; Wang et al., 2014). Among these methods, the fossil plant stomatal ratio (*SR*)-based method has been widely used in CO_2 estimates reconstruction from Paleozoic to Cenozoic. In recent years, an increasing number of mathematical models for pCO_2 reconstruction have been proposed and widely used, such as the mechanistic CO_2 model proposed by Franks (2014) (Konrad et al., 2008; Franks et al., 2014; Konrad et al., 2017). The advantage of this mechanism model is that it can be used to estimate the paleo-CO_2 in any period from the Devonian to the present, and it is considered to be more sensitive at high pCO_2 (Franks et al., 2014; Royer et al., 2019). Furthermore, with the continuous updating of the methods, increasing attention has been given to the error analysis, and the requirements for the pCO_2 reconstruction accuracy are also increasing. The pCO_2 estimates based on multiple species are generally thought to be more effective than the pCO_2 estimates based on single species to reduce the range of error (Reichgelt and D'Andrea, 2019).

In this study, we selected the well-preserved leaves of *Brachyphyllum* and *Cupressinocladus* from the Lower Cretaceous of the Laiyang Basin, and used three methods: the *SR*-based method, mechanistic model and carbon-isotope model, to reconstruct the pCO_2 during the Hauterivian–Barremian (Early Cretaceous). Moreover, a greater insight into the relationship between the pCO_2 concentration and the Weissert event during the Early Cretaceous is discussed.

https://doi.org/10.5194/cp-2021-96
Preprint. Discussion started: 24 August 2021

Climate of the Past Discussions
Open Access
EGU

2. Material and methods

2.1. Geological and stratigraphical settings

The Laiyang Basin refers to the Mesozoic depression in the Laiyang area of Shandong Province, and this Mesozoic depression is located on the north side of the Sulu orogenic belt and the east of the North China Craton (Luo et al., 1990; Li and Zhang, 2000; Jin et al., 2018; Fig. 1A, B). The Cretaceous strata from this basin are well-developed, continuously exposed and complete and contain abundant and various fossil categories (Luo et al., 1990; Li and Zhang, 2000; Jin et al., 2018). This area is one of the most desirable areas for studying the geologic evolution of Asia in the Cretaceous (Luo et al., 1990; Li and Zhang, 2000). The Laiyang Basin developed mainly the Lower Cretaceous Laiyang Formation, the Qingshan Formation, and the Upper Cretaceous Wangshi Formation, which do not conform to the underlying strata of the Proterozoic Jingshan Group, the Archean Jiaodong Group or the overlying strata of Paleogene (Luo et al., 1990; Fig. 1A, B). According to the various lithological characteristics, sedimentary cycles and fossil beds, the Laiyang Formation is divided into four members (Luo et al., 1990). The third member is the main fossiliferous layer of the Laiyang Formation. The total thickness of this member is 181 to 472 metres, and most of the area is approximately 400 m, which is composed mainly of shale and sandstone and contains small amounts of carbonate sediments (Fig. 1C). Current fossils have also been collected from this member in the Huangyadi–Beibozi profile (Fig. 1C).

https://doi.org/10.5194/cp-2021-96
Preprint. Discussion started: 24 August 2021

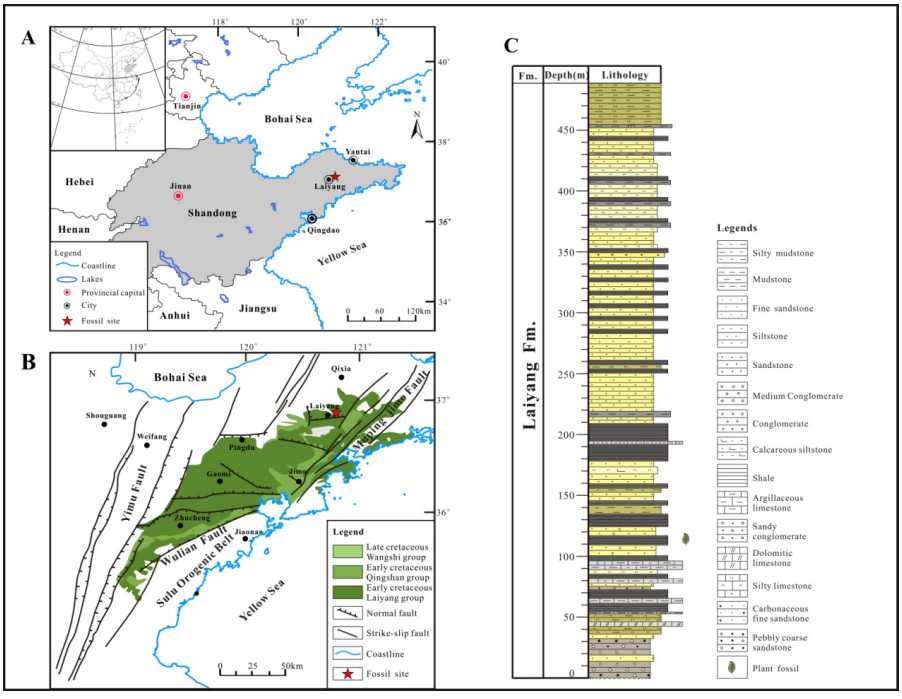

Fig. 1. A) Location of the fossil site and the tectonic units of the Laiyang Basin; B) Stratigraphic section of the Early Cretaceous Laiyang Formation, Laiyang Basin and the fossil–bearing horizon.

Various paleoentomologists have conducted detailed studies on the geological age of the Laiyang Formation (Luo et al., 1990; Lin, 1995; Hong, 1998; Ren and Hong, 1998; Zhang, 2003; Grimaldi and Engel, 2005; Zhang and Rasnitsyn, 2006). Now the point of view that the Laiyang Formation belongs to the Early Cretaceous has been accepted by most researchers (Chen et al., 1980; Luo et al., 1983). The significant SHRIMP U-Pb age shown by the tuff in the basal conglomerates of the Laiyang Group confirms that the age of the Laiyang Group is in the range of 120–149 Ma (Early Cretaceous) (Zhang et al., 2018). According to the $^{40}Ar/^{39}Ar$ age of hornblende and the U-Pb dating of zircons by many researchers, the maximum deposition age of the Laiyang Formation is approximately 130 Ma in the Hauterivian–Barremian (the early stage of the Early Cretaceous) (Ling et al., 2007; Zhang et al., 2008; Xie et al., 2012; Huo et al., 2015; O'Reilly et al., 2015). Therefore, the Laiyang Formation belongs to the Early Cretaceous, and the stratigraphic position of the current fossils is assigned to the Hauterivian–Barremian.

2.2. Fossil materials and living relatives

https://doi.org/10.5194/cp-2021-96
Preprint. Discussion started: 24 August 2021

Climate of the Past Discussions
Open Access
EGU

112 2.2.1 Description of the fossil species

113 In our study, two fossil species from two plant families were recorded in the Laiyang
114 Formation in the Laiyang Basin: *Brachyphyllum obtusum* Chow et Tsao (family Cheirolepidiaceae)
115 and *Cupressinocladus* sp. (family Cupressaceae). *Brachyphyllum obtusum* is characterized by
116 incomplete twigs up to 3-4 mm wide with spirally disposed scale-like leaves (Fig. 2F–I). Leaves
117 are adpressed and imbricate, broad rhomboidal in face view, approximately 2.5-2.7 mm wide and
118 2-3.4 mm long (Fig. 2F–I). The leaf margin is entire, and the apex is relatively obtuse, with a
119 mucro at the top. A single midvein is prominent on the abaxial leaf surface. The leaf cuticles are
120 amphistomatic (Fig. 2F–I). The abaxial cuticle is very thick, and the stomata are arranged in
121 longitudinal rows all over the surface (Fig. 3F–I). Each row is separated by 5-10 abaxial epidermal
122 cells. Ordinary epidermal cells are rectangular or irregular polygonal, with strongly thickened and
123 straight anticlinal walls and well-developed papillae. Stomatal complexes are rounded or narrowly
124 rounded in outline, haplocheilic and monocyclic. The guard cells are sunken and generally
125 surrounded by 4-6 subsidiary cells that form a ring. The epidermal cells and stomata of the adaxial
126 cuticle are similar to those of the abaxial cuticle.

https://doi.org/10.5194/cp-2021-96
Preprint. Discussion started: 24 August 2021

Climate of the Past Discussions

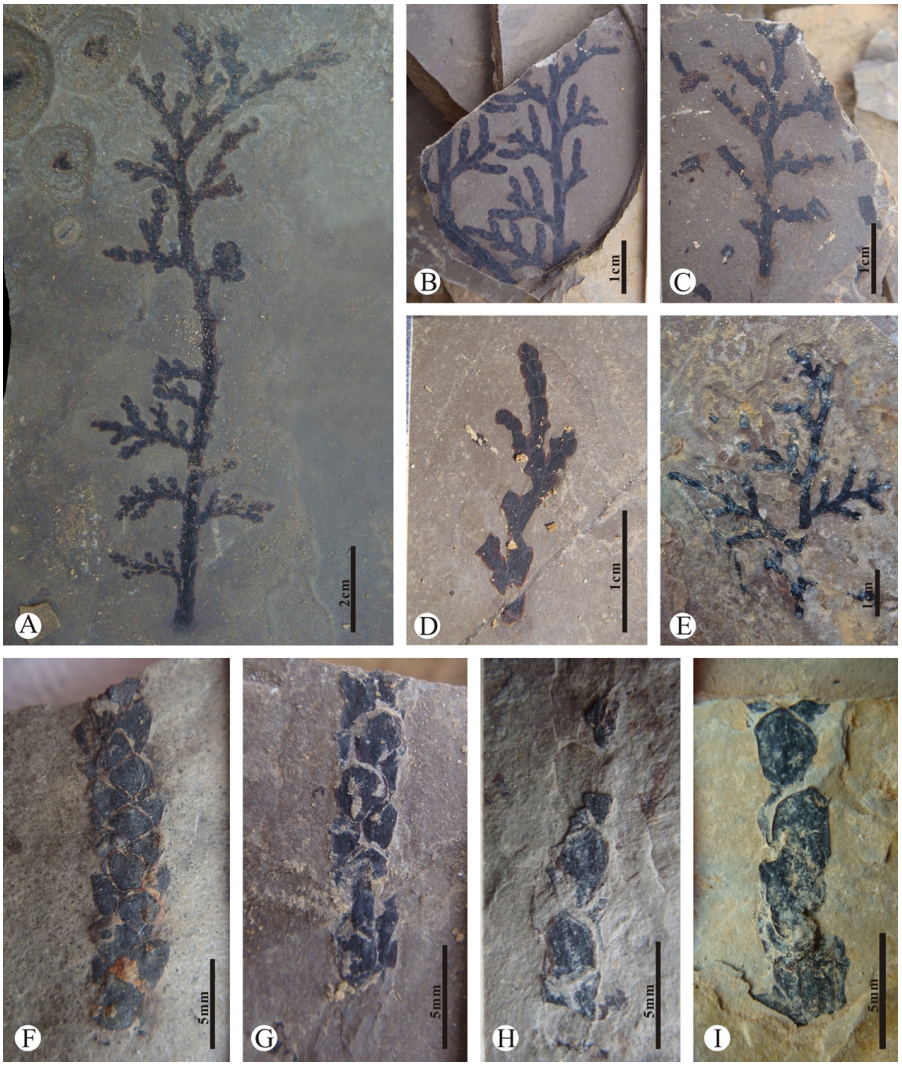

Fig. 2. Morphological structures of *Cupressinocladus* and *Brachyphyllum* from the Lower Cretaceous of the Laiyang Basin. A–E, *Cupressinocladus* sp. (Specimen No: A, LDGSW–2016–508A; B, LDGSW–2016–1401; C, LDGSW–2015–501A; D, LDGSW–2016–462A; E, LDGSW–2015–907); F–I, *Brachyphyllum obtusum* (Specimen No: F, LDGSW–2015–154A; B, LDGSW–2015–159B; C, LDGSW–2015–162A; D, LDGSW–2015–178A).

https://doi.org/10.5194/cp-2021-96
Preprint. Discussion started: 24 August 2021

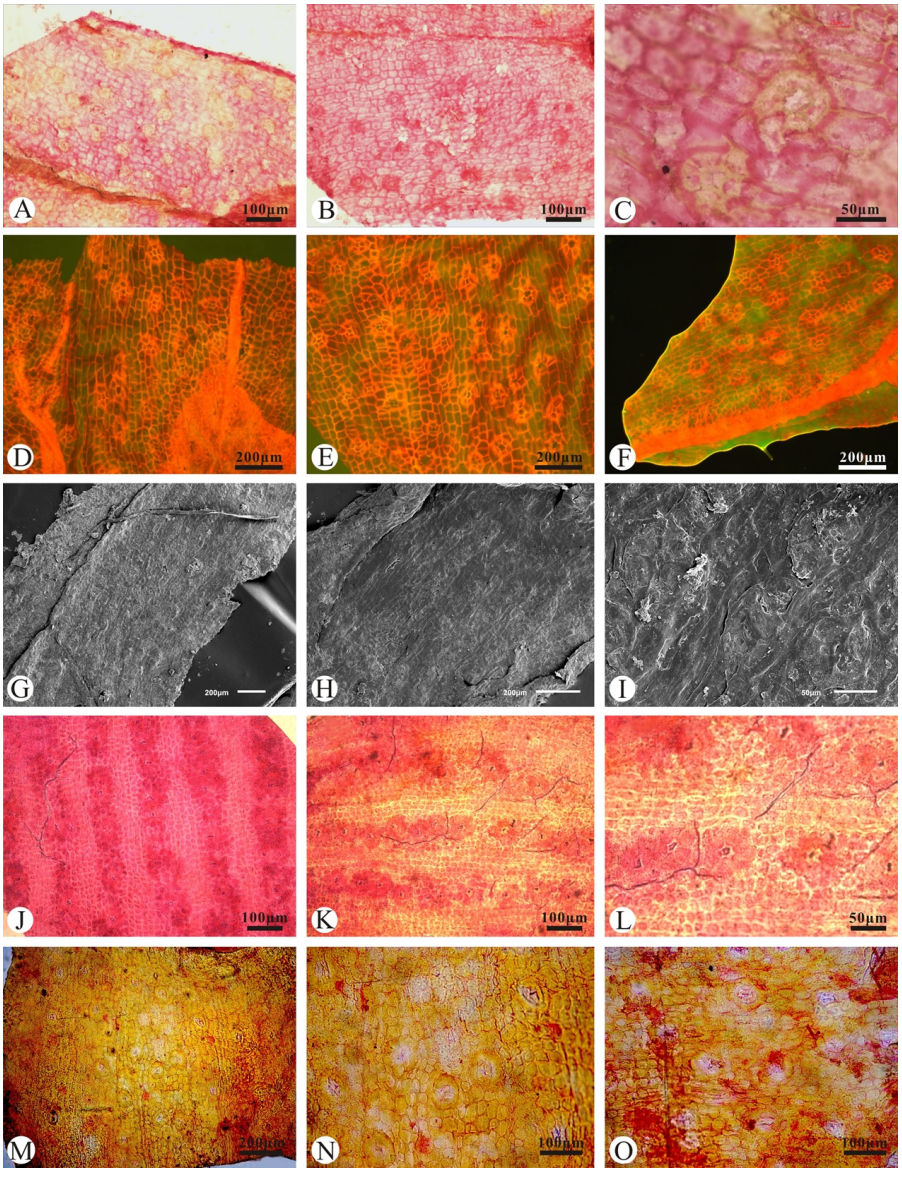

Fig. 3. Cuticular structures of *Cupressinocladus* and *Brachyphyllum* from the Lower Cretaceous of the Laiyang Basin. A, B, Abaxial cuticle of *Cupressinocladus* sp. under stereomicroscope showing epidermal cells and stomata; scale bar 100 μm; C, The detail of stomatal showing guard and subsidiary cells of *Cupressinocladus* sp. abaxial cuticle; scale bar 50 μm; D–F, Abaxial leaf cuticle of *Cupressinocladus* sp. under fluorescence microscope showing epidermal cells and stomata; scale bar 200 μm; G, H, Adaxial cuticle of *Cupressinocladus* sp. under SEM showing epidermal cells and stomata; scale bar 200 μm; I, The detail of stomatal under SEM showing

https://doi.org/10.5194/cp-2021-96
Preprint. Discussion started: 24 August 2021


Climate of the Past Discussions

guard and subsidiary cells of *Cupressinocladus* sp. adaxial cuticle; scale bar 50 μm; J, K, Abaxial cuticle of *Brachyphyllum obtusum* under stereomicroscope showing epidermal cells and stomata; scale bar 100 μm; I, The detail of stomatal under stereomicroscope showing guard and subsidiary cells of *Brachyphyllum obtusum* abaxial cuticle; scale bar 50 μm; M–O, Adaxial cuticle of *Brachyphyllum obtusum* under stereomicroscope showing epidermal cells and stomata; M, Scale bar 200 μm; N, O, Scale bar 100 μm.

Cupressinocladus sp. preserved as last-second or last-third leafy twigs. The leaves on ultimate leafy shoots are sessile, decussate and imbricate arranged. The base of the leaves is decurrent and partly concealed by the leaves of the lower pair. The lateral leaves are conduplicate and oval, with the entire margin and obtuse apical tip, approximately 1.7-2.5 mm long and 0.8-1.2 mm wide in the exposed part. The facial leaves are rhombic at the exposed part, without keels, appressed to the shoot axis. The leaves on last-third leafy shoots are ovate to broadly lanceolate, approximately 2.3–5.2 mm long and 1–1.4 mm wide. The leaf cuticles are amphistomatic. The stomata on the adaxial cuticle are arranged in longitudinal rows all over the surface. Each row is separated by 4–6 epidermal cells, and a small number of stomata are irregularly distributed. The epidermal cells between the two bands are rectangular, with straight anticlinal walls and well-developed papillae, approximately 65–89 μm long and 27–41 μm wide. The epidermal cells in rows are short rectangular or irregular polygonal with papillae. Stomatal complexes are rounded or elliptic, haplocheilic, monocyclic. The guard cells are sunken and generally surrounded by 5-6 subsidiary cells with papillae. The abaxial cuticle epidermal cells and stomata are similar to those of the adaxial cuticle.

2.2.2. Selection of nearest living equivalents (NLEs)

Numerous studies have already discussed the nearest living equivalent species (NLEs) of *Brachyphyllum* (Cheirolepidiaceae), the most common of which are *Athrotaxis cupressoides* (9.0 ± 1.5), *Tetraclinis articulate* (11.7 ± 1.1), *Calocedrus decurrens* (9.9 ± 1.4), *Callitris columnaris* (8.9 ± 1.6), and *Callitris rhomboidea* (8.2 ± 1.4) as NLEs of *Brachyphyllum* to restore the pCO_2 during the Cretaceous period (McElwain and Chaloner, 1996; Haworth et al. 2005; Haworth et al., 2010). Hence, we also selected these five species as NLEs of *B. obtusum*, and took their average value of 9.5 ± 1.4 as the stomatal index (*SI*) of NLEs of *B. obtusum*.

Many leafy-shoots assignable to the *Cupressinocladus* have been reported from the Mesozoic strata in Europe and Asia (Florin, 1958, 1963; Harris, 1969; Miller, 1977; Shi et al., 2011; Jin et al., 2017). These leafy shoots resemble in external appearance the leafy shoots of extant Cupressaceae, but as far as their leaf-cuticle is concerned, many of the leafy shoots belong to the

https://doi.org/10.5194/cp-2021-96
Preprint. Discussion started: 24 August 2021


Climate of the Past Discussions

extinct family Cheirolepidiaceae, such as *Cupressinocladus obatae* and *Cupressinocladus ramonensis* (OKUBO and KIMURA, 1991; Srinivasan, 1995). The external appearances of the present species *Cupressinocladus* sp. is very similar to the external appearances of Cupressaceae, whereas the stomata are distributed all over the surface of the leaves, and the leaves do not form stomatal bands. Such stomatal distribution has also has been seen in the Cheirolepidiaceae conifers. In addition, two adjacent stomata often share a single subsidiary cell in cupressaceous conifers, but such characteristics have has not been observed in the present species *C.* sp. and other cheirolepidiaceous conifers (except in *Pseudofrenelopsis parceramosa*, *Glenrosa pagiophylloides*, *Glenrosa texensis*, *Glenrosa falcate* and *Glenrosa virginiensis*) (Watson, 1977; Watson and Fisher, 1984; Srinivasan, 1992; Gomez et al., 2012). To date, as far as the cuticular features mentioned above are concerned, the present species more resembles to Cheirolepidiacea. Based on the similarities of ecology and morphology, the extant *Athrotaxis cupressoides*, *Tetraclinis articulate*, *Calocedrus decurrens*, *Callitris columnaris*, *Callitris rhomboidea* and *Salicornia virginica* have been selected as the NLEs of the extinct Cheirolepidiaceae conifers by numerous researchers (McElwain and Chaloner, 1996; Haworth et al. 2005; Haworth et al., 2010). Among these conifers, *Tetraclinis articulate*, *Calocedrus decurrens*, *Callitris columnaris*, *Callitris rhomboidea* also belong to Cupressaceae, and the external appearance of these four speciesis are similar to the external appearance of the present leafy-shoots. Therefore, we select these four species as NLEs of *C.* sp., and take their average value 9.7 ± 1.5 as the *SI* of NLEs of *C.* sp..

2.3. Proxy models and methods

2.3.1 *SR*-based method

McElwain and Chaloner (1995) proposed the *SR*-based method and the conception of "the nearest living equivalent (NLE)". NLE refers to the living species that share similar ecoenvironments and functional structures with fossil plants (McElwain, 1998; Chen et al., 2001). NLE is applied mainly in the comparison of the stomatal parameters between living and fossil plants and then to reconstruct the pCO_2 semiquantitatively (McElwain, 1998; Chen et al., 2001). Four parameters need to be calculated when using *SR*-based method in pCO_2 reconstruction: stomatal density (*SD*), epidermal density (*ED*), *SI* and *SR*, and detailed descriptions of all the parameters and equations involved are listed in Table 1. This method was standardized by McElwain and Chaloner (1996) and McElwain (1998) with two standardizations: carboniferous standardization ($1SR=2RCO_2$) and recent standardization ($1SR=1.2RCO_2$). Carboniferous standardization has been found to be most appropriate for pCO_2 reconstruction based on the Paleozoic and Mesozoic taxa, whereas recent standardization is more applicable to the pCO_2

https://doi.org/10.5194/cp-2021-96
Preprint. Discussion started: 24 August 2021

Climate of the Past Discussions

reconstruction of Cenozoic taxa (Steinthorsdottir et al., 2011; Steinthorsdottir et al., 2013; Steinthorsdottir and Vajda, 2015). Here, we used both standardizations to obtain the minimum and maximum paleo-CO_2 estimates. The relation between pCO_2 and stomatal parameters can be expressed by the equation pCO_2 (ppmv) $=SR\times300$.

Table 1 Parameters required by the SR-based method.

Parameter	Unit	Description
SD	mm^{-2}	Stomatal density, the number of stomata in unit area (mm^2)
ED	mm^{-2}	Epidermal density, the number of epidermic cells in unit area (mm^2)
SI	%	Stomatal index, the percentage of stomata to the total number of stomata and epidermal cells, $SI=SD/(SD+ED)\times100$
SR	-	Stomatal ratio, the stomata index ratio between the NLEs and fossil species, $SR=SI_{NLEs}/SI_{fossil}$
SI_{NLEs}	%	The stomatal index of the NLEs
SI_{fossil}	%	The stomatal index of the fossil species
RCO_2	-	The ratio of the paleo-CO_2 concentration over the pre-industrial revolution level (approximately 300 ppmv)

2.3.2 The mechanistic model

Recently, the mechanistic model based on leaf gas exchange has been widely applied to obtain the pCO_2 during the Mesozoic and Paleozoic (Konrad et al., 2008; Franks et al., 2013; Franks et al., 2014; Konrad et al., 2017; Du et al., 2018; Li et al., 2019; Zhou et al., 2020). The precondition of mechanistic model is to assume that the exchange conditions and forms of gases in the photosynthesis of the ancient forest are the same as those of the living forest (Franks et al. 2014). The change in paleoatmospheric CO_2 concentration (C_a) would influence the diffusion rate of the CO_2 from the atmosphere to the fixation part (stomata) in the leaf (Franks et al. 2014). In turn, the diffusion rate influences the CO_2 assimilation rate (A_n) in organisms (Franks et al. 2014). This mechanistic model estimates the concentration of atmospheric CO_2 by iteratively solving the equations (1)–(7) in Fig.4 based on three parameters, including A_n (the assimilation rate of plant leaves towards CO_2, which can be calculated by estimating A_0), $g_{c(tot)}$ (the total operational conductance to CO_2 diffusion) and C_i/C_a (the ratio of leaf internal CO_2 concentration to C_a) (Farquhar et al., 1980; Farquhar et al., 1982; Farquhar et al., 1989; Franks et al., 2009; Franks et al. 2013; Franks et al. 2014).

https://doi.org/10.5194/cp-2021-96
Preprint. Discussion started: 24 August 2021

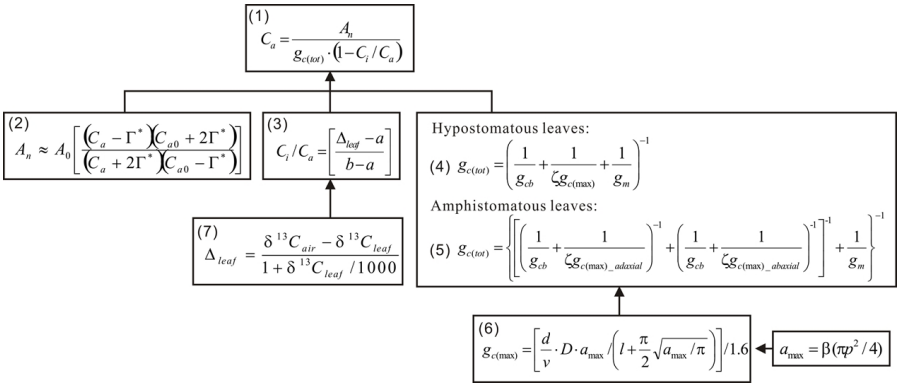

Fig. 4. The main equation and procedures of the mechanistic model based on Franks et al. (2014). All parameters and their description are listed on Table 2.

Table 2 Parameters required by the mechanistic model based on Franks et al. (2014)

Parameter	Unit	Description
C_i	mol m^{-3}	Leaf internal CO_2
C_a	ppmv(mol m^{-3})	Atmospheric CO_2
A_n	μmol m^{-2} s^{-1}	The CO_2 assimilation rate
$g_{c(tot)}$	mol m^{-2} s^{-1}	The total operational conductance to CO_2 diffusion
g_{cb}	mol m^{-2} s^{-1}	Leaf boundary layer conductance to CO_2, 2.0 mol m^{-2} s^{-1} (Collate et al., 1991)
$g_{c(op)}$	mol m^{-2} s^{-1}	Operational stomatal conductance
g_m	mol m^{-2} s^{-1}	The mesophyll conductance, derived from Epron et al. 1995, Evans and Von Caemmerer, 1996
$g_{c(max)}$	mol m^{-2} s^{-1}	The Maximum of $g_{c(op)}$ (When the stomata opening is the largest)
ζ	–	The ratio of operational stomatal conductance to maximum stomatal conductance, 0.2 (Franks et al., 2009)
a_{max}	m^2	Maximum area of stomatal pore for maximally open stoma
l	μm	Stomatal pore depth
p	μm	Stomatal pore length
d/v	mol m^{-1} s^{-1}	The ratio of diffusivity of CO_2 in air to molar volume of air, 9.40096 × 10^{-5} mol m^{-1} s^{-1} (Franks and Beerling, 2009)
SD	mm^{-2}	Stomatal density
β	–	Maximum pore area/area of circle with diameter, 0.5 (Franks et al., 2014)
$\delta^{13}C_{leaf}$	‰	Carbon isotope composition of fossil leaves, measurements on fossil leaves
$\delta^{13}C_{air}$	‰	Carbon isotope composition of palaeoatmosphere
Δ_{leaf}	‰	The carbon isotope discrimination by the plant
a	‰	The carbon isotope fractionation due to diffusion of CO_2 in air, 4.4‰ (Von Caemmerer, 2000)

https://doi.org/10.5194/cp-2021-96
Preprint. Discussion started: 24 August 2021

Climate of the Past Discussions

b	‰	The fractionation associated with RuBP carboxylase, 30‰ (Von Caemmerer, 2000)
A_0	μmol m^{-2} s^{-1}	Reference CO_2 assimilation rate at ambient, 10μmol m^{-2} s^{-1} (Franks et al. 2014)
C_{a0}	ppmv	Assigned to correspond approximately with A_0, 360 ppmv (Franks et al., 2014)
Γ*	μmol mol^{-1}	CO_2 compensation point in the absence of dark respiration, 40 μmol mol^{-1} (25℃) (Franks et al., 2014)

A_n can be obtained by equation (2), which is derived from an expression for Ru-BP regeneration-limited photosynthesis (Farquhar et al., 1980). In this equation, A_0 and C_{a0} are the reference values of A_n and C_a of the four groups under general environmental conditions. The plants analysed in this paper all belong to the conifer group. Therefore, A_0 and C_{a0} take values of 10 μmol $m^{-2}s^{-1}$ and 360 ppmv respectively (Franks et al. 2014). $g_{c(tot)}$ is composed of three main components: g_{cb} (2 $mol^{-1}s^{-1}$), $g_{c(max)}$ and g_m. For trees that grow naturally under external conditions, the ζ value is usually approximately 0.2. Equation (4) is the standard form for $g_{c(tot)}$ of hypostomatous leaves (Franks et al. 2014). For amphistomatous leaves the term $((1/g_{cb}) + (1/\zeta g_{c(max)}))^{-1}$ must be calculated separately for the adaxial and abaxial leaf surfaces ($g_{c(max)\_adaxial}$ and $g_{c(max)\_abaxial}$ are the maximum stomatal conductance to CO_2 of the adaxial and abaxial leaf surfaces, respectively), added together in parallel, and then added in series with g_m to obtain $g_{c(tot)}$ (equation (5); Franks et al. 2014; Fig.4). $g_{c(max)}$ is obtained by basic diffusion equations (6) by measuring l (stomatal pore depth) and SD (stomatal density) of the fossil plant. a_{max} determines the length of the stomatal pore (p): $a_{max} = \beta(\pi p^2/4)$, in which the β values of pteridophytes and gymnosperms are usually 0.5 (Franks et al., 2014). C_i/C_a can be obtained by measuring the relative carbon isotope composition of the fossil leaves ($\delta^{13}C_{leaf}$) (see equations (3) and (7)). In equation (7), Δ_{leaf} (‰) can be obtained by the analysis of $\delta^{13}C_{leaf}$ and translation of $\delta^{13}C_{air}$, both of which were introduced later in this study.

This model has been described and discussed in detail by Franks et al. (2014). Thus, only a brief introduction is presented here, and detailed descriptions of all the parameters involved are listed in Table 2. The calculation of Ca (pCO_2) and other variables was performed by the R program, which was provided by Franks et al. (2014).

2.3.3 Carbon isotope model

Carbon isotopes of plant fossils are relevant tools for describing past carbon cycle and CO_2 dynamics (Schubert and Jahren, 2012; Franks et al., 2014; Barral et al., 2017b; Barral et al., 2017a). Atmospheric CO_2 is the main source of carbon assimilated by plants via photosynthesis

https://doi.org/10.5194/cp-2021-96
Preprint. Discussion started: 24 August 2021


Climate of the Past Discussions
Open Access
EGU

(Barral et al., 2017a). These theories make it possible to use the carbon isotope composition of plant fossils to analyse the evolution of atmospheric pCO_2 during past periods. Schubert and Jahren (2012) established a carbon isotope model (equation (8), r=0.9) relating pCO_2 to $\delta^{13}C_{leaf}$ to reconstruct the pCO_2 concentration.

.

$$\Delta^{13}C_{leaf} = \frac{(28.26)(0.22)(pCO_2 + 23.9)}{28.26 + (0.22)(pCO_2 + 23.9)} \quad (8)$$

$\Delta^{13}C_{leaf}$ values (carbon isotope fractionation by plants) were estimated from $\delta^{13}C_{leaf}$ and concomitant $\delta^{13}C_{CO2}$ values by using equation (9) (Farquhar et al., 1982).

$$\Delta^{13}C_{leaf} = \frac{\delta^{13}C_{CO_2} - \delta^{13}C_{leaf}}{1 + \delta^{13}C_{leaf}/1000} \quad (9)$$

Where $\delta^{13}C_{leaf}$ is the carbon isotope composition of leaves of fossil plants and $\delta^{13}C_{CO2}$ is the carbon isotope composition of atmospheric CO_2 during the geological period (Farquhar et al., 1982). The $\delta^{13}C_{CO2}$ during the Hauterivian–Barremian is taken as an average value of -5.78‰ in this paper, which is based on the $\delta^{13}C_{CO2}$ reconstructed by Barral et al (2017a) from the carbon isotope value of marine carbonate.

2.3.4. Fossil cuticle proxy measurements

The fossil cuticles were removed from rock using tweezers and a needle and then immersed in a 10% hydrochloric acid (HCl) solution for 24 h. After being washed a few times with distilled water, the cuticle samples were immersed in a 50% hydrofluoric acid (HF) solution for 24 h and then treated with Schulze solution for a few minutes to hours until the cuticle turned yellow and translucent. The abaxial and adaxial cuticles were separated using a needle under a dissection microscope. The isolated cuticles were washed with distilled water and gently brushed several times until the cuticle was clean. Some cuticle samples were mounted on slides, embedded in glycerin jelly, and sealed with Canadian balsam. The cuticle slides were observed under a Zeiss AXO-40 microscope, and some cuticle samples were mounted on stubs, coated with gold and examined under an SEM (scanning electron microscope, JEOL JSM–5600LV) at Lanzhou University, China.

We used 16 cuticle samples of *Cupressinocladus* sp. and 14 cuticle samples of *B. obtusum* (120 samples in total) for paleo-CO_2 analysis. All cuticle parameters (e.g. stomatal density, stomatal index, stomatal/pore length, stomatal width) were counted within 0.09 mm_2 squares, and Photoshop CS8 software was used for at least 5 counts for each specimen. All leaf-level measurements and paleo-CO_2 estimates are presented Table 3–5. For each proxy method, 95% confidence intervals for estimated CO_2 were determined using 10,000 Monte Carlo simulations

https://doi.org/10.5194/cp-2021-96
Preprint. Discussion started: 24 August 2021

Climate of the Past Discussions
Open Access
EGU

(Table 3–5, Fig. 6) to propagate uncertainties in all input parameters.

The carbon stable isotopes were measured at Key Laboratory of Petroleum Resources, Northwest Institute of Eco-Environment and Resources, Chinese Academy of Sciences (Lanzhou, China). The fossil leaf samples were removed and treated with 10% HCl for 24 h and then washed multiple times with distilled water until neutral. Next the fossil leaf samples were treated with 50% HF for 24 h and rinsed again. Finally, the fossil leaf samples were dried in a drying oven at 40 °C for 24 h, and their $\delta^{13}C_{leaf}$ was measured with a Flash 2000 HT Elemental Analyser connected to a Thermo Fisher MAT-253 mass spectrometer. The fossil leaf samples were normalized to the Pee Dee Belemnite (PDB) standard with an analysis precision of ±0.3‰, using IAEA-600 caffeine as a certified reference material. The carbon isotopic composition of atmospheric CO_2 ($\delta^{13}C_{air}$) (which was used in the Franks' model) is obtained by $\delta^{13}C_{leaf}$ from the equation $\delta^{13}C_{air} = (\delta^{13}C_{leaf} + 18.67) /1.10$ (Arens et al., 2000).

4. Results and Discussion

4.1. Results and comparison across methods

The pCO_2 in the Laiyang Basin during the Hauterivian–Barremian was reconstructed by two fossil coniferous species (*Cupressinocladus* sp. and *Brachyphyllum obtusum*) based on the *SR* method, mechanistic model and carbon isotope model. Using the *SR*-based method, the *SI* and *SR* values of our fossil specimens were measured and calculated, and the estimated pCO_2 results were in the range of 579 to 663 ppmv based on recent standardization and between 966 and 1106 ppmv based on carboniferous standardization (Table 3; Fig. 5A). Using the mechanistic model, the mean results of pCO_2 ranged from 472 to 525 ppmv, which is lower than the estimated results based on the *SR*-based method (Table 4; Fig. 5A). The carbon isotope model contributed the lowest value of pCO_2, which ranged from 202 to 409 ppmv (Table 5; Fig. 5A).

https://doi.org/10.5194/cp-2021-96
Preprint. Discussion started: 24 August 2021

Climate of the Past Discussions
Open Access
EGU

324 **Table 3** Stomatal parameters of *Brachyphyllum* and *Cupressinocladus* from Laiyang Basin
325 during Hauterivian-Barremian, and estimated pCO_2 values based on the SR-based method.

Taxon	Specimen number	*ED* (mm^{-2})	*SD* (mm^{-2})	*SI* (%)	*SR*	Carboniferous standardization		Recent standardization	
						RCO_2	pCO_2 (ppmv)	RCO_2	pCO_2 (ppmv)
Cupressinocladus sp.	LDGSW–2016–508A	1619.6	94.6	5.5	1.8	3.5	1054.4	2.1	632.7
		1418.9	77.0	5.1	1.9	3.8	1131.3	2.3	678.8
		1598.7	86.6	5.1	1.9	3.8	1132.7	2.3	679.6
		1591.8	86.4	5.1	1.9	3.8	1130.3	2.3	678.2
	LDGSW–2016–462A	1316.2	65.0	4.7	2.1	4.1	1236.8	2.5	742.1
		1211.5	68.4	5.3	1.8	3.6	1088.7	2.2	653.2
		1871.2	96.0	4.9	2.0	4.0	1193.1	2.4	715.9
	LDGSW–2016–1401	2515.0	124.3	4.7	2.1	4.1	1235.6	2.5	741.4
		2477.4	126.6	4.9	2.0	4.0	1196.7	2.4	718.0
		2384.2	118.6	4.7	2.0	4.1	1228.3	2.5	737.0
		2019.0	110.9	5.2	1.9	3.7	1117.4	2.2	670.5
	LDGSW–2015–487A	1613.7	92.8	5.4	1.8	3.6	1070.4	2.1	642.2
	LDGSW–2015–501A	1213.5	85.6	6.6	1.5	2.9	883.0	1.8	529.8
	LDGSW–2015–907	1009.1	59.8	5.6	1.7	3.5	1040.3	2.1	624.2
		1114.5	76.4	6.4	1.5	3.0	907.3	1.8	544.4
		1978.2	116.6	5.6	1.7	3.5	1045.2	2.1	627.1
	Average value	1684.5 ±216.0	92.9 ±9.5	5.3± 0.2	1.8± 0.1	3.7± 0.2	1105.7 ±47.4	2.2±0.1	663.4 ±28.4
Brachyphyllum obtusum	LDGSW–2016–162A	1878.8	112.7	5.7	1.7	3.4	1007.0	2.0	604.2
		1847.8	105.6	5.4	1.8	3.5	1054.5	2.1	632.7
	LDGSW–2016–385	1414.6	79.2	5.3	1.8	3.6	1074.9	2.1	644.9
		1991.3	111.9	5.3	1.8	3.6	1071.1	2.1	642.7
	LDGSW–2016–154A	2564.6	131.5	4.9	1.9	3.9	1168.5	2.3	701.1
		1927.7	132.5	6.4	1.5	3.0	886.1	1.8	531.7
		1891.7	122.3	6.1	1.6	3.1	938.7	1.9	563.2
	LDGSW–2015–143	1467.2	111.3	7.1	1.3	2.7	808.4	1.6	485.0
		1991.3	111.9	5.3	1.8	3.6	1071.1	2.1	642.7
	LDGSW–2016–178A	1663.9	103.7	5.9	1.6	3.2	971.6	1.9	583.0
		1548.0	139.3	8.3	1.2	2.3	690.3	1.4	414.2
		1772.7	119.8	6.3	1.5	3.0	900.6	1.8	540.4
	LDGSW–2016–159B	2098.6	118.5	5.3	1.8	3.6	1066.2	2.1	639.7
	Average value	1823.2 ±102.3	115.1 ±4.9	6.0± 0.3	1.6± 0.1	3.2± 0.1	965.5± 44.5	1.9±0.1	579.3 ±26.7

https://doi.org/10.5194/cp-2021-96
Preprint. Discussion started: 24 August 2021

Climate of the Past Discussions
Open Access
EGU

Table 4 Stomatal data and carbon isotope data of *Brachyphyllum* and *Cupressinocladus* from Laiyang Basin, and estimated pCO_2 value based on the mechanistic model. SN=specimen number; *l*_ad=*l*_adaxial (μm); *el*_ad=*el*_adaxial (μm); *p*_ad=*p*_adaxial (μm); *ep*_ad=*ep*_adaxial (μm); *l*_ab=*l*_abaxial (μm); *el*_ab=*el*_abaxial (μm); *p*_ab=*p*_abaxial (μm); *ep*_ab=*ep*_abaxial (μm); $\delta=\delta^{13}C$ (‰); $\delta_a=\delta^{13}C_{air}$ (‰); *SD* (mm^{-2}); a_{max} (m^2); $G=g_{c(max)}$ (mol m^{-2} s^{-1}); G1ab=$g_{c(op)}$_abaxial (mol m^{-2} s^{-1}); G2=$g_{c(tot)}$ (mol m^{-2} s^{-1}); C= C_i/C_a; A_n (μmol m^{-2} s^{-1}); P=Ca /pCO_2 (ppmv).

Taxon	SN	*l*_ad	*el*_ad	*p*_ad	*ep*_ad	*l*_ab	*el*_ab	*p*_ab	*ep*_ab	δ	δ_a	*SD*	a_{max}	G	G1ab	G2	C	A_n	P
Cupressinocladus sp.	LDGS-W-2016-580A	13.0	1.6	19.6	3.8	13.7	0.8	24.4	6.2	26.9	7.5	86.6	1.37×10^{-10}	0.30	0.06	0.06	0.61	10.6	441
		11.4	1.0	19.1	3.3	15.7	0.8	21.4	7.2	26.9	7.5	86.4	2.38×10^{-10}	0.40	0.07	0.05	0.61	10.7	463
		12.0	0.4	20.5	1.4	13.9	2.2	26.2	3.2	26.9	7.5	94.6	2.35×10^{-10}	0.51	0.12	0.06	0.61	10.3	406
		9.7	0.1	10.7	2.8	12.4	1.1	19.2	2.0	26.9	7.5	77.0	1.12×10^{-10}	0.22	0.04	0.04	0.61	11.3	620
	LDGS-W-2016-462A	10.1	1.6	25.2	3.5	10.2	0.9	20.4	4.0	26.9	6.5	96.0	2.98×10^{-10}	0.67	0.13	0.06	0.58	10.1	368
		9.4	0.8	18.3	4.7	10.2	2.6	19.5	1.6	26.9	6.5	65.0	1.21×10^{-10}	0.17	0.03	0.05	0.58	10.9	503
		9.5	1.3	18.7	4.1	9.1	1.2	21.3	3.6	26.9	6.5	68.4	2.51×10^{-10}	0.43	0.07	0.05	0.58	10.6	455
	LDGS-W-2016-1401	10.5	1.1	28.1	5.8	10.1	1.3	25.8	3.4	27.5	8.0	124.3	2.66×10^{-10}	0.88	0.18	0.07	0.63	10.0	365
		10.2	0.7	29.1	2.3	10.3	1.2	24.7	3.3	27.5	8.0	126.6	1.34×10^{-10}	0.52	0.11	0.07	0.63	10.0	361
		9.7	1.5	20.8	3.4	9.0	1.4	23.7	4.4	27.5	8.0	118.6	3.10×10^{-10}	0.93	0.18	0.07	0.63	10.2	391
		8.3	0.5	21.5	1.5	10.1	0.4	25.7	4.1	27.5	8.0	110.9	1.71×10^{-10}	0.51	0.11	0.07	0.63	10.2	390
	LDGS-W-2015-907	8.7	0.8	7.2	2.6	10.4	1.8	12.7	2.1	27.1	7.7	59.8	7.42×10^{-11}	0.14	0.02	0.02	0.62	12.4	116
		8.7	5.7	7.4	4.4	4.9	1.4	13.3	3.6	27.1	7.7	76.4	1.61×10^{-11}	0.08	0.01	0.04	0.62	11.5	684
		9.1	1.6	8.2	2.1	10.1	1.5	10.0	1.6	27.1	7.7	116.6	4.35×10^{-11}	0.18	0.03	0.04	0.62	11.7	736
	Average value	10.0	1.0	18.5	3.2	10.1	1.4	20.6	3.7	27.0	7.6	93.4	1.72×10^{-10}	0.43	0.08	0.05	0.61	10.8	525
Brachyphyllum obtusum	LDGS-W-2016-162A	9.5	0.5	15.6	2.5	10.9	1.4	22.5	6.9	23.1	4.0	112.7	4.36×10^{-11}	0.14	0.03	0.06	0.60	10.3	402
		10.1	0.4	15.0	0.6	7.3	0.3	12.3	4.2	23.1	4.0	105.6	1.16×10^{-10}	0.43	0.08	0.05	0.60	10.9	501
	LDGS	9.5	0.5	14.0	0.8	8.1	1.4	14.7	7.2	23.1	4.0	79.2	$7.79\times10^{-}$	0.21	0.03	0.05	0.0	11.3	591

https://doi.org/10.5194/cp-2021-96
Preprint. Discussion started: 24 August 2021

Climate of the Past Discussions
Open Access
EGU

	W–	7	6	.7	5	7	6	.9	1	.9	8		10^{-11}	8	9	2	63	7	
	2016–	10	0.	15	0.	8.	1.	11	6.	23	4.	111.	4.51×	0.22	0.04	0.05	0.	11.1	530
	385	.2	2	.4	6	3	1	.7	6	.9	8	9	10^{-11}	2	8	6	63	6	
	LDGS	5.	0.	9.	2.	7.	1.	15	5.	22	3.	131.	2.77×	0.17	0.03	0.06	0.	10.4	417
	W–	7	2	6	9	8	5	.2	9	.8	8	5	10^{-11}	6	3	0	59	9	
	2016–	8.	0.	19	5.	7.	1.	9.	3.	22	3.	132.	7.09×	0.36	0.06	0.06	0.	10.4	403
	154A	6	9	.8	1	7	9	2	0	.8	8	5	10^{-11}	2	6	1	59	2	
		7.	0.	11	4.	6.	0.	9.	1.	22	3.	122.	2.05×	0.14	0.02	0.05	0.	11.0	537
		8	8	.2	5	5	8	9	2	.8	8	3	10^{-11}	2	8	0	59	7	
	LDGS	8.	0.	18	3.	9.	0.	21	6.	23	4.	118.	1.38×	0.48	0.09	0.06	0.	10.3	395
	W–	6	7	.7	2	6	9	.2	8	.6	5	5	10^{-10}	1	8	7	62	6	
	2016–																		
	159B																		
	Average	8.	0.	15	2.	8.	1.	14	5.	23	4.	114.	6.74×	0.27	0.05	0.05	0.	10.7	472
	value	8	5	.0	5	3	2	.6	2	.3	2	3	10^{-11}	3	4	8	61	8	

https://doi.org/10.5194/cp-2021-96
Preprint. Discussion started: 24 August 2021

Climate of the Past Discussions
Open Access
EGU

334 Table 5 The carbon isotope parameters of *Brachyphyllum* and *Cupressinocladus* from Laiyang

Taxon	Specimen number	$\delta^{13}C$ (‰)	$\delta^{13}C_{CO2}$(‰)	$\Delta^{13}C_{leaf}$	pCO_2(ppmv)
Cupressinocladus	LDGSW–2016–580A	-26.90	-5.78	21.70	401
sp.	LDGSW–2016–462A	-26.30	-5.78	21.07	353
	LDGSW–2016–1401	-27.50	-5.78	22.33	460
	LDGSW–2015–907	-27.10	-5.78	21.91	420
	Average value	-26.95	-5.78	21.76	409
Brachyphyllum	LDGSW–2016–162A	-23.10	-5.78	17.73	192
obtusum	LDGSW–2016–385	-23.90	-5.78	18.56	222
	LDGSW–2016–154A	-22.80	-5.78	17.42	182
	LDGSW–2016–159B	-23.60	-5.78	18.25	210
	Average value	-23.35	-5.78	17.99	202

335 Basin, and estimated pCO_2 values based on the carbon isotope model.

336

https://doi.org/10.5194/cp-2021-96
Preprint. Discussion started: 24 August 2021

Climate of the Past Discussions
Open Access
EGU

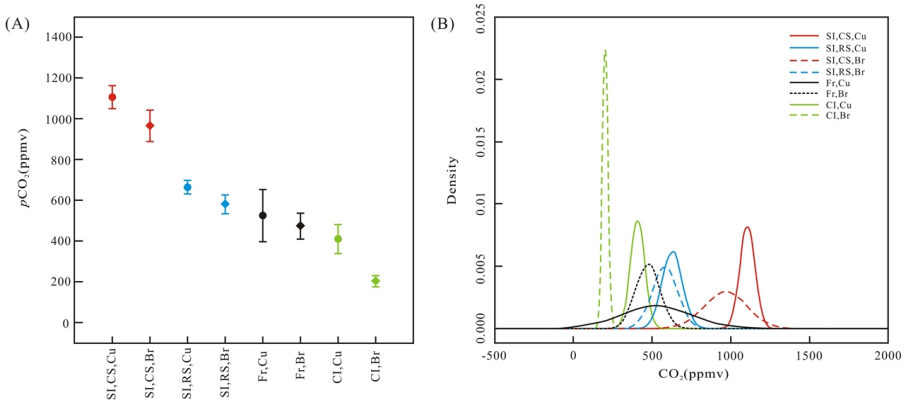

Fig. 5. A, The pCO_2 ranges during the Early Cretaceous (Hauterivian-Barremian); The error bars indicate the 95% confidence interval for each pCO_2 estimate; B, Probability distributions from all proxy estimates; SI, CS, Cu= *SR*-based method based on carboniferous standardization, *Cupressinocladus* sp.; SI, CS, Br= *SR*-based method based on carboniferous standardization, *Brachyphyllum obtusum*; SI, RS, Cu= *SR*-based method based on recent standardization, *Cupressinocladus* sp.; SI, RS, Br= *SR*-based method based on recent standardization, *Brachyphyllum obtusum*; Fr, Cu= mechanistic model based on *Cupressinocladus* sp.; Fr, Br= mechanistic model based on *Brachyphyllum obtusum*; CI, Cu= carbon isotope model based on *Cupressinocladus* sp.; CI, Br= carbon isotope model based on *Brachyphyllum obtusum*.

Based on the probability distributions from all proxy estimates, we note that most of the 95% confidence intervals of the recent standardization from SR-based method and mechanistic model overlap (Fig. 5B). However, the confidence interval of the carboniferous standardization from the *SR*-based method is much higher than the confidence interval of all other methods. The traditional method of using plant fossil *SI* to reconstruct pCO_2 has the following disadvantages. First, the *SI* has specific responses to CO_2 concentration, so the quantitative estimation of pCO_2 is limited to specific fossil species that are close to existing taxa (Küaschner et al., 2008). We must assume that these species have not suffered ecological and physiological evolution over time. However, this assumption has been questioned. Second, the response of the fitting function between *SI* and pCO_2 is nonlinear, and the gradient decreases with increasing CO_2 concentration. Therefore, it is difficult to calculate the accurate pCO_2 value by the fitting function when the CO_2 concentration in the environment is higher than the CO_2 concentration of the current environment (Beerling and Royer, 2002a; Beerling et al., 2009). Third, the traditional *SR*-based method depends mainly on the density of stomata and epidermal cells, without the change of stomatal length, while many experiments show that the change of stomatal length is often related to the atmospheric CO_2

https://doi.org/10.5194/cp-2021-96
Preprint. Discussion started: 24 August 2021


Climate of the Past Discussions
Open Access
EGU

363 concentration (Konrad et al., 2008; Franks and Beerling, 2009). Finally, the statistical requirement
364 of *SI* in this method is that epidermal cells should be clearly identified. However, due to the
365 influence of other epidermal structures (hair base, glands, etc.), it is difficult to obtain reliable
366 epidermal cell data for many plant fossils (Grein et al., 2013).

367 The error between the estimated value and the measured value of the mechanical model used
368 in this paper is 2.6%, and its accuracy is significantly higher than the accuracy of other
369 reconstruction methods (Franks et al. 2014). In addition, the mechanical model avoids some of the
370 abovementioned drawbacks of the traditional *SR*-based method for estimating the pCO_2 and fully
371 considers the influence of key parameters in gas exchange on the reconstruction results (such as
372 the length and depth of the stomatal pores, the maximum opening area of the stoma, and the
373 carbon isotope) (Franks et al. 2014). Therefore, this model has a strong reference when used to
374 reconstruct the pCO_2 in the geological period. We also see that the 95% confidence intervals of
375 the pCO_2 value estimated by two different plants of *Cupressinocladus* sp. and *B. obtusum* using
376 the same method are highly coincident, increasing both accuracy and precision (Fig. 5B). We note
377 that the 95% confidence interval of the pCO_2 value obtained by *Cupressinocladus* sp. in the
378 mechanical model is larger than the other 95% confidence interval, possibly due to the uncertainty
379 of the value of A_n (Fig. 5B). Therefore, when using the mechanical model to estimate the pCO_2
380 value, selecting A_n values of species with similar habits is more appropriate (Reichgelt and
381 D′Andrea, 2019).

382 We note that the CO_2 estimate from the carbon isotope model is lower than the estimates
383 from the *SR*-based method and mechanical model. The main reason is that the main parameter
384 settings of the carbon isotope model are based on environmental factors since the Quaternary and
385 plants′ own factors (Schubert and Jahren, 2012, 2015). However, the main parameters of the
386 Quaternary are still used in reconstructing the pCO_2 value of the Cretaceous, and whether this is
387 reasonable still requires much data to verify.

388 Finally, we note that during the Hauterivian–Barremian (the early period of the Early
389 Cretaceous), the pCO_2 value was generally low, and it is feasible to use the mechanical model to
390 restore pCO_2. In addition, the interval of the pCO_2 value which is obtained by the mechanical
391 model is larger (443–693 ppm), and the pCO_2 value shows greater instability, possibly because the
392 mechanical model is established based on living plants. Most of the biological anatomical
393 parameters in the model, such as the thickness of the assimilation tissue and the conductivity of
394 the liquid part in the mesophyll, must be borrowed from the existing closest relatives of fossil
395 plants. Therefore, using this model will produce certain errors when recovering paleoclimate
396 parameters. According to the *SR*-based method, the pCO_2 value estimated by *Brachyphyllum*

https://doi.org/10.5194/cp-2021-96
Preprint. Discussion started: 24 August 2021

Climate of the Past Discussions
Open Access
EGU

obtusum (approximately 557–945 ppm) is lower than the pCO_2 value estimated by *Cupressinocladus* sp. (approximately 599–1252 ppm). This obvious difference may be due to the different responses of different plants to CO_2 concentrations.

4.2 Comparison with other pCO_2 records for the Early Cretaceous

The reconstruction methods of pCO_2 during the Hauterivian–Barremian (Early Cretaceous) include mainly calculations with plant fossil stomatal data (Haworth et al., 2005; Du et al., 2016; Aucour et al., 2008; Sun et al., 2016; Passalia, 2009), isotope analysis (Heimhofer et al., 2004; Wallmann, 2001; Ekart et al., 1999; Fletcher et al., 2005), biogeochemical models etc (Berner, 1994; Tajika, 1999; Berner and Kothavala, 2001; Rothman, 2002; Hansen and Wallman, 2003; Bergman, 2004). The pCO_2 value of the Hauterivian–Barremian obtained in this paper is generally low, which is close to most of the pCO_2 that was restored in the Early Cretaceous (Table 6; Fig. 6). For example, the pCO_2 values reconstructed by Haworth et al. (2005) based on the SR-based method ($SI_{(NLES)}$ = 10.5, *Pseudofrenelopsis parceramosa*) are approximately 653–1089 ppmv (Early Hauterivian), 630–1050 ppmv (Late Hauterivian), 568–946 ppmv (Early Barremian) and 641–1068 ppmv (late Barremian). The Late Hauterivian pCO_2 reconstructed by Dai and Sun (2018) based on the SR-based method ($SI_{(NLES)}$ = 5.8, *Pseudofrenelopsis parceramosa*) is approximately 595–946 ppmv. Both of these results are highly coincident with the pCO_2 value obtained by the SR-based method in this paper. The pCO_2 from the mechanical model in this paper is similar to the late Barremian pCO_2 (395–789 ppmv) obtained by Retallack (2009a) using *Ginkgo* fossils and also similar to early Barremian pCO_2 (560 ppmv) estimated by Robinson et al. (2002) using stable isotopes of calcareous conglomerates from southern England. Huang et al. (2012) also believed that pCO_2 during Berriasian-Barremian was low based on the paleosol carbonate, and the late Barremian pCO_2 was about 365–644 ppmv. This value is also similar to the results recovered by the recent standardization of the *SR*-based method and the mechanistic model in this paper.

https://doi.org/10.5194/cp-2021-96
Preprint. Discussion started: 24 August 2021

Climate of the Past Discussions
Open Access
EGU

423 **Table 6** Estimated pCO_2 during the early stage of Early Cretaceous.

Age	Proxy	*SI* (fossil) (%)	pCO_2 (ppmv)	Locality	Data sources
SR-based method					
Berriasian	*Ginkgo coriacea*	3.79±0.22-4.75±0.32	918–1920	China, Inner Mongolia, Huolinghe	Sun et al., 2007
Valanginian–Hauterivian	*Gingko coriacea*	3.4±0.1	740	China, Inner Mongolia, Huolinghe	Chen et al., 2001
Hauterivian–Barremian	*Cupressinocladus* sp.	5.3±0.2	663–1105	China, Shandong	This study
	Brachyphyllum obtusum	6.0±0.3	579–965	China, Shandong	This study
Early Hauterivian	*Pseudofrenelopsis parceramosa*	5.8 ±1.3	653–1089	UK, USA	Haworth et al., 2005
Late Hauterivian	*Pseudofrenelopsis parceramosa*	6.0 ±1.3	630–1050	UK, USA	Haworth et al., 2005
	Pseudofrenelopsis papillosa	5.8±0.5	595–957	China, Fujian	Dai and Sun, 2018
Early Barremian	*Pseudofrenelopsis parceramosa*	6.6 ±1.3	568–946	UK, USA	Haworth et al., 2005
Late Barremian	*Pseudofrenelopsis parceramosa*	5.9 ±1.0	641–1068	UK, USA	Haworth et al., 2005
	Frenelopsis alata	4.6±0.6	700–1400	Argentina	Aucour et al., 2008; Passalia, 2009
	Ginkgo	–	395–789	USA	Retallack, 2009a,b
Barremian–Aptian	*Ginkgo*	–	400–3510	USA	Retallack, 2009a,b
Mechanistic model					
Berriasian–Valanginian	*Otozamites ornatus*	–	416	Patagonia, Argentina	De Seoane, 2001; Franks et al., 2014
Hauterivian–Barremian	*Cupressinocladus* sp.	–	432–691	China, Shandong	This study
	Brachyphyllum obtusum	–	371–817	China, Shandong	This study
Other carbon isotope analysis					
Early-middle Berriasian	Paleosol carbonates	–	287–389	China	Huang et al., 2012
Early Valanginian	Paleosol carbonates	–	237–245	China	Huang et al., 2012
Hauterivian–Barremian	Carbon isotope of *Brachyphyllum*	–	409	China, Shandong	This study
	Carbon isotope of	–	202	China,	This study

https://doi.org/10.5194/cp-2021-96
Preprint. Discussion started: 24 August 2021

Climate of the Past Discussions
Open Access
EGU

	Cupressinocladus			Shandong	
Hauterivian/Aptian–Albian	Paleosol carbonates	–	2300	Japan, Korea	Lee et al., 1999
Early Barremian	Calcrete nodules	–	560	UK	Robinson et al., 2002
Late Barremian	Paleosol carbonates	–	365–644	China	Huang et al., 2012

424

https://doi.org/10.5194/cp-2021-96
Preprint. Discussion started: 24 August 2021

Climate of the Past Discussions
Open Access
EGU

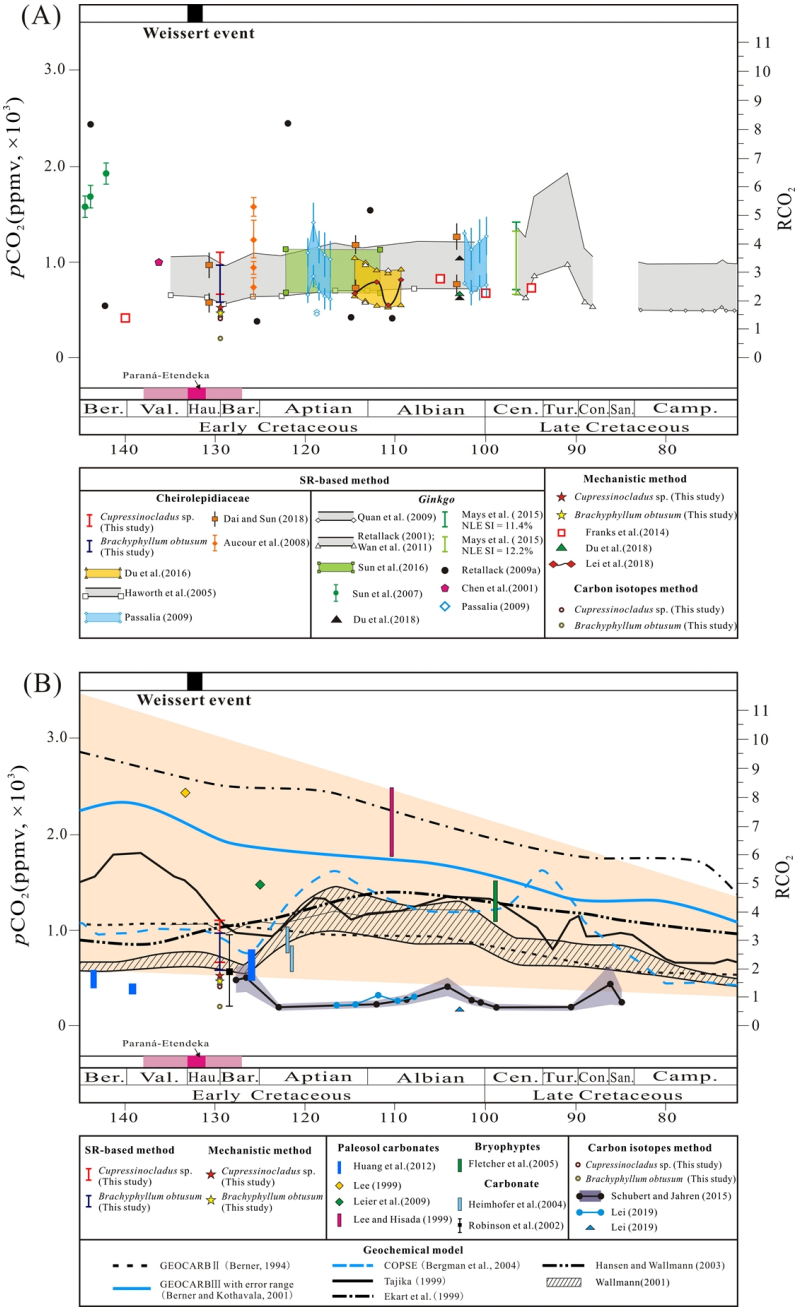

425

426 **Fig. 6.** A: Our estimated pCO_2 values during Hauterivian–Barremian (Early Cretaceous), and
427 previous data based on *SR*-based method and mechanistic model; B: Our estimated pCO_2 values
428 during Hauterivian–Barremian, and previous data based on biogeochemical models and carbon
429 isotopes.

https://doi.org/10.5194/cp-2021-96
Preprint. Discussion started: 24 August 2021


Climate of the Past Discussions
Open Access
EGU

430

431 Furthermore, the global carbon cycle model established by Tajika (1999) and Wallmann
432 (2001) and the geochemical model COPSE established by Bergman et al. (2004) both show that
433 pCO_2 during the Hauterivian–Barremian was relatively low compared with other pCO_2 values of
434 the Early Cretaceous. The pCO_2 obtained by the recent standardization of the *SR*-based method
435 and the mechanistic model in this paper are close to the value of the Hauterivian–Barremian
436 recovered by Hansen and Wallmann (2003). However, the pCO_2 value estimated by the
437 carboniferous standardization of the *SR*-based method is slightly higher, which is closer to the
438 concentration curves obtained from the geochemical models GEOCARB II, COPSE and Tajika
439 (1999) (Fig. 6).

440 Schubert and Jahren (2015) reconstructed pCO_2 and its changes during the past 30,000 years
441 based on the carbon isotope model with a large amount of global terrestrial organic matter and
442 carbon isotopic composition of plant fossils. The reconstruction results are consistent with the
443 results known from ice cores (Schubert and Jahren, 2015). The pCO_2 during the Barremian–
444 Santonian Cretaceous reconstructed by Barral et al. (2017a) with the plant carbon isotope model is
445 about 185–502 ppmv, which is generally lower than the results from plant stomatal method,
446 isotope method, biogeochemical model, etc (Fig. 6). Furthermore, the pCO_2 value reconstructed in
447 this paper based on the carbon isotope method during the Hauterivian–Barremian is also lower
448 than the results of the *SR*-based method and the mechanistic model and close to the results of
449 Barral et al (2017a) (Fig. 6). Therefore, in combination with previous studies, the pCO_2 values
450 reconstructed from the carbon isotope model are generally lower than the pCO_2 values
451 reconstructed from other methods.

452

453 4.3. The pCO_2 records and Weissert event

454 Strata of the Valanginian age (Early Cretaceous, 139.8–132.9 Ma) record a 1.5‰ positive
455 carbon-isotope excursion (CIE), the Weissert event, which is regarded as a global perturbation of
456 coupled oceanic and atmospheric carbon reservoirs based on the wide documentation from marine
457 bulkrock and belemnite carbonates and fossil wood organic matter (Lini et al., 1992; Wortmann
458 and Weissert, 2000; Weissert and Erba, 2004; Gröcke et al., 2005; Price et al., 2018; Jelby et al.,
459 2020). The latest estimate of the timing of the onset of the Weissert event is ascertained to be
460 135.22 ± 1 Ma derived from U-Pb ages from tuff layers in the Neuquén Basin and an update of the
461 Valanginian–Hauterivian astrochronological time scale (Aguirre-Urreta et al., 2015; Martinez et
462 al., 2015). Most studies have confirmed that the Valanginian Weissert event coincided with the
463 onset of the eruptive phase of the Paraná-Etendeka, which has recently been dated between

https://doi.org/10.5194/cp-2021-96
Preprint. Discussion started: 24 August 2021


Climate of the Past Discussions

134.6 ± 0.6 Ma and 134.3 ± 0.8 Ma (Price et al., 2018).

The intense volcanism in the geological age affected seawater chemistry in different ways. The widely dispersed volcanic emissions formed by Paraná-Etendeka volcanic activity possibly caused increased concentrations of toxic trace metals in the surface ocean, affecting marine primary producers (Möller et al. , 2020). Following the positive carbon isotope excursion of the Weissert event, fertilization of the oceans increased, which caused sequestration of marine organic carbon (Erba et al., 2004; Duchamp-Alphonse et al., 2007). Then the weathering of basalt gradually strengthened, which eventually led to a decrease in the pCO_2 and global temperature in the last stages of the Weissert event (the late Valanginian) (Möller et al., 2020). This cooling event has been inferred based on glendonite occurrences from the Canadian Arctic Archipelago, ice rafted debris in central Australia, belemnites and fish tooth enamel $\delta^{18}O$ data from northern Germany, Western Siberia, northern Italy, France and Spain (Kemper and Schmitz, 1981; Frakes and Francis, 1988; Podlaha et al., 1998; Price and Mutterlose, 2004; Weissert and Erba, 2004; McArthur et al., 2007; Bodin et al., 2015; Meissner et al., 2015; Price et al., 2018; Möller et al. , 2020).

Most of the pCO_2 values that have been recovered thus far all reflect the significant decrease during the Hauterivian–Barremian, such as the pCO_2 values obtained from *SR*-based method of *Pseudofrenelopsis parceramosa*, the geochemical model COPSE, and the global carbon cycle model established by Tajika (1999) and Wallmann (2001), all of the Hauterivian–Barremian pCO_2 values obtained from these studies reached the lowest point in Early Cretaceous (Tajika, 1999; Wallmann, 2001; Bergman et al., 2004; Haworth et al., 2005). Similarly, the Hauterivian–Barremian pCO_2 values in Laiyang Basin reconstructed by both fossil coniferous species (*C.* sp. and *B. obtusum*) from each method are relatively low compared with other pCO_2 values in the Early Cretaceous. All of these pCO_2 records also reflect the cooling event in the final stage of the Weissert event.

5. Conclusions

In this study, we present a new pCO_2 record for the Hauterivian–Barremian on the basis of fossil leaves (*Cupressinocladus* sp. and *Brachyphyllum obtusum*) collected from Laiyang Basin. All the required fossil cuticle and isotopic parameters were measured and three different proxy methods were applied to estimate pCO_2. The pCO_2 values estimated using the SR-based method were approximately 579–663 ppmv calibrated with recent standardization and 966–1106 ppmv calibrated with carboniferous standardization. The pCO_2 value estimated using the mechanistic model was about 472–525 ppmv. The pCO_2 value estimated using the carbon isotope model was approximately 472–525 ppmv. By summarizing the pCO_2 record estimated using *SR*-based,

https://doi.org/10.5194/cp-2021-96
Preprint. Discussion started: 24 August 2021


Climate of the Past Discussions

499 mechanistic, and carbon isotope model, the pCO_2 variability was discussed. The mechanistic
500 model may be widely applied to more fossil taxa than the *SR*-based method and retains sensitivity
501 at high pCO_2. The pCO_2 value obtained from this study indicates a relatively low atmospheric CO_2
502 concentration and a cool climate during the Hauterivian–Barremian, which also reflects the
503 response of terrestrial plants to the cooling event in the last stages of the Weissert event.
504
505 **Author contributions**
506 All authors contributed to obtaining and analysing the data utilised in the study. Zhang
507 Mingzheng, Du Baoxia and Sun Bainian conceived the research. Lei Xiangtong contributed the
508 mechanistic model analyses. Dong Junling performed fossil cuticles analyses. Jin Peihong wrote
509 the paper. All authors contributed to improving and editing the paper, and they are in agreement
510 with the content of manuscript.
511
512 **Competing interests**
513 We declare that we have no financial and personal relationships with other people or
514 organizations that can inappropriately influence our work.
515
516 **Acknowledgments**
517 We are very grateful to the editor and anonymous reviewers for useful comments that
518 significantly improved the manuscript.
519
520 **Financial support**
521 This study was supported by the Second Tibetan Plateau Scientific Expedition and Research
522 Program (STEP) (Grant No. 2019QZKK0704), the National Natural Science Foundation of China
523 (No. 41902017), the Natural Science Foundation of Gansu Province (No. 2021000050), the Key
524 Laboratory Project of Gansu Province (No. SZDKFJJ20201208), and State Key Laboratory of
525 Palaeobiology and Stratigraphy (Nanjing Institute of Geology and Palaeontology, CAS) (No.
526 203103).
527
528
529 **References**
530
531 Aguirre-Urreta, B., Lescano, M., Schmitz, M.D., Tunik, M., Concheyro, A., Rawson, P.F., Ramos,
532 V.A.: Filling the gap: new precise Early Cretaceous radioisotopic ages from the Andes,
533 Geol. Mag., 152, 557–564, https://doi.org/10.1017/S001675681400082X, 2015.
534 Arens, N.C., Jahrens, A.H., Amundson, R.: Can C_3 plants faithfully record the carbon isotopic

https://doi.org/10.5194/cp-2021-96
Preprint. Discussion started: 24 August 2021

composition of atmospheric carbon dioxide? Palaeobiology, 26, 137–164, https://doi.org/10.1666/0094-8373(2000)026<0137:CCPFRT>2.0.CO;2, 2000.

Aucour, A.M., Gomez, B., Sheppard, S.M.F., Thevenard, F.: $\delta^{13}C$ and stomatal number variability in the Cretaceous conifer *Frenelopsis*, Palaeogeography, Palaeoclimatology, Palaeoecology, 257, 462–473, https://doi.org/10.1016/j.palaeo.2007.10.027, 2008.

Barclay, R.S., Mcelwain, J.C., Sageman, B.B.: Carbon sequestration activated by a volcanic CO_2 pulse during Ocean Anoxic Event 2, Nature Geoscience, 3, 205–208, doi:10.1038/ngeo757, 2010.

Barral, A., Gomez, B., Fourel, F., Daviero-Gomez, V., Lécuyer, C.: CO_2 and temperature decoupling at the million-year scale during the Cretaceous Greenhouse, Scientific Reports, 7, 8310, DOI:10.1038/s41598-017-08234-0, 2017a.

Barral, A., Gomez, B., Legendre, S., Lécuyer, C.: Evolution of the carbon isotope composition of atmospheric CO_2 throughout the Cretaceous, Palaeogeography, Palaeoclimatology, Palaeoecology, 471, 40–47, https://doi.org/10.1016/j.palaeo.2017.01.034, 2017b.

Beerling, D.J., Fox, A., Anderson, C.W.: Quantitative uncertainty analyses of ancient atmospheric CO_2 estimates from fossil leaves, American Journal of Science, 309, 775–787, https://doi.org/10.2475/09.2009.01, 2009.

Beerling, D.J., Osborne, C., Chaloner, W.: Evolution of leaf–form in land plants linked to atmospheric CO_2 decline in the Late Palaeozoic era, Nature, 410, 352–354, https://doi.org/10.1038/35066546, 2001.

Beerling, D.J., Royer, D.L.: Fossil plants as indicators of the Phanerozoic global carbon cycle, Annual Review of Earth and Planetary Sciences, 30, 527–556, https://doi.org/10.1146/annurev.earth.30.091201.141413, 2002a.

Beerling, D.J., Royer, D.L.: Reading a CO_2 signal from fossil stomata, New Phytologist, 153, 387–397, https://doi.org/10.1046/j.0028-646X.2001.00335.x, 2002b.

Bergman, N.M., Lenton, T.M., Watson, A.J.: COPSE: a new model of biogeochemical cycling over Phanerozoic time, American Journal of Science, 304, 397–437, 2004.

Berner, R.A.: GEOCARB II: a revised model of atmospheric CO_2 over Phanerozoictime, Am. J. Sci., 294, 56–91, https://doi.org/10.2475/ajs.304.5.397, 1994.

Berner, R.A., Kothavala, Z.: GEOCARB III: revised model of atmospheric CO_2 over Phanerozoic time, Am. J. Sci., 301, 182–204, https://doi.org/10.2475/ajs.301.2.182, 2001.

Bodin, S., Meissner, P., Janssen, N.M.M., Steuber, T., Mutterlose, J.: Large igneous provinces and organic carbon burial: Controls on global temperature and continental weathering during the Early Cretaceous, Glob. Planet. Chang., 133, 238–253, https://doi.org/10.1016/j.gloplacha.2015.09.001, 2015

Boucot, A.J., Gray, J.: A critique of Phanerozoic climatic models involving changes in the CO_2 content of the atmosphere, Earth Sci. Rev., 56 (1–4), 1–159, https://doi.org/10.1016/S0012-8252(01)00066-6, 2001.

Chen, L.Q., Li, C.S., Chaloner, W.G., Beerling, D.J., Sun, Q.G., Collinson, M.E., Mitchell, P.L.: Assessing the potentialfor the stomatal characters of extant and fossil *Ginkgo* leaves tosignal atmospheric CO_2 change, American Journal of Botany, 88, 1309–1315, https://doi.org/10.2307/3558342, 2001.

Chen, P.J., Cao, M.Z., Pan, H.Z., Ye, C.H., Li, W.B., Shen, Y.B., Chen, J.H.: Issues of continental strata in Mesozoic from Shandong, Journal of Stratigraphy, 4 (4), 301–309, 1980.

https://doi.org/10.5194/cp-2021-96
Preprint. Discussion started: 24 August 2021

579 Dai, J., Sun, B.N.: Early Cretaceous atmospheric CO_2 estimates based on stomatal index of
580 Pseudofrenelopsis papillosa (Cheirolepidiaceae) from southeast China, Cretaceous
581 Research, 85, 232–242, https://doi.org/10.1016/j.cretres.2017.08.011, 2018.
582 De Seoane, L.V.: Cuticular study of Bennettitales from the Springhill Formation, Lower Cretaceous of
583 Patagonia, Argentina, Cretaceous Research, 22, 461–479,
584 https://doi.org/10.1006/cres.2001.0266, 2001.
585 Du, B.X., Lei, X.T., Zhang, M.Z., Wang, S., Li, A.J., Du, Z., Xing, W.W.: Late early Cretaceous
586 climate and pCO_2 estimates in the Liupanshan Basin, northwest China, Palaeogeography,
587 Palaeoclimatology, Palaeoecology, 503, 26–39,
588 https://doi.org/10.1016/j.palaeo.2018.04.023, 2018.
589 Du, B.X., Sun, B.N., Zhang, M.Z., Yang, G.L., Xing, L.T., Tang, F.J., Bai, Y.X.: Atmospheric
590 palaeo-CO_2 estimates based on the carbon isotope and stomatal data of Cheirolepidiaceae
591 from the Lower Cretaceous of the Jiuquan Basin, Gansu Province, Cretaceous Research,
592 62, 142–153, https://doi.org/10.1016/j.cretres.2015.07.020, 2016.
593 Duchamp-Alphonse, S., Fiet, N., Adatte, T., Pagel, M.: Climate and sea-level variations along the
594 northwestern Tethyan margin during the Valanginian C-isotope excursion:
595 Mineralogical evidence from the Vocontian Basin (SE France), Palaeogeography,
596 Palaeoclimatology, Palaeoecology, 302, 243–254,
597 https://doi.org/10.1016/j.palaeo.2011.01.015, 2011.
598 Ekart, D.D., Cerling, T.E., Montanez, I.P., Tabor, N.J.: A 400 million year carbon isotope record
599 of pedogenic carbonate: implications for paleoatmospheric carbon dioxide, American
600 Journal of Science, 299, 805–827,
601 http://earth.geology.yale.edu/~ajs/1999/10.1999.01Ekart, 1999.
602 Erba E., Bartolini A., Larson R.L.: Valanginian Weissert oceanic anoxic event, Geology, 32, 149–
603 152, https://doi.org/10.1130/G20008.1, 2004.
604 Farquhar, G.D., And, J.R.E., Hubick, K.T.: Carbon Isotope Discrimination and Photosynthesis,
605 Annu. Rev. Plant Physiol. Plant Mol. Biol., 40, 503–537,
606 https://doi.org/10.1146/annurev.pp.40.060189.002443, 1989.
607 Farquhar, G.D., Caemmerer, S.V., Berry, J.A.: A biochemical model of photosynthetic CO_2
608 assimilation in leaves of C_3 species, Planta, 149, 78–90, doi: 0032-
609 0935/80/0149/0078/$02.60, 1980.
610 Farquhar, G.D., O'leary, M.H., Berry, J.A.: On the Relationship Between Carbon Isotope
611 Discrimination and the Intercellular Carbon Dioxide Concentration in Leaves, Functional
612 Plant Biology, 9, 281–292, https://doi.org/10.1071/PP9820121, 1982.
613 Fletcher, B.J., Beerling, D.J., Brentnall, S.J., Royer, D.L.: Fossil bryophytes as recorders of
614 ancient CO_2 levels: experimental evidence and a Cretaceous case study, Glob.
615 Biogeochem. Cycles, 19, 1–13, https://doi.org/10.1029/2005GB002495, 2005.
616 Fletcher, B.J., Brentnall, S.J., Anderson, C.W., Berner, R.A., Beerling, D.J.: Atmospheric carbon
617 dioxide linked with Mesozoic and early Cenozoic climate change, Nature Geoscience, 1,
618 43–48, doi:10.1038/ngeo.2007.29, 2008.
619 Florin, R.: On Jurassic taxads and conifers from north-western Europe and eastern Greenland,
620 Acta Horti Bergiani, 17, 257–402, 1958.
621 Florin, R.: The distribution of conifer and taxad genera in time and space, Acta Horti Bergiani,
622 20(4), 121–312, 1963.

https://doi.org/10.5194/cp-2021-96
Preprint. Discussion started: 24 August 2021

623 Föllmi, K.B.: Early Cretaceous life, climate and anoxia, Cretaceous Research, 35, 230–257,
624 https://doi.org/10.1016/j.cretres.2011.12.005, 2012.
625 Frakes, L.A., Francis, J.E.: A guide to Phanerozoic cold polar climates from highlatitude ice-
626 rafting in the Cretaceous, Nature, 333, 547–549, https://doi.org/10.1038/333547a0,
627 1988.
628 Franks, P.J., Adams, M.A., Amthor, J.S., Barbour, M.M., Berry, J.A., Ellsworth, D.S., Farquhar,
629 G.D., Ghannoum, O., Loyd, J.L., McDowell, N., Norby, R.J., Tissue, D.T., Caemmerer,
630 S.: Sensitivity of plants to changing atmospheric CO_2 concentration: from the geological
631 past to the next century, New Phytol, 197, 1077–1094, https://doi.org/10.1111/nph.12104,
632 2013.
633 Franks, P.J., Drake, P.L., Beerling, D.J.: Plasticity in maximum stomatal conductance constrained
634 by negative correlation between stomatal size and density: an analysis using Eucalyptus
635 globules, Plant Cell Environ., 32, 1737–1748, https://doi.org/10.1111/j.1365-
636 3040.2009.002031.x, 2009.
637 Franks, P.J., Royer, D.L., Beerling, D.J., Van de Water, P.K., Cantrill, D.J., Barbour, M.M., Berry,
638 J.A.: New constraints on atmospheric CO_2 concentration for the Phanerozoic,
639 Geophysical Research Letters, 41, 4685–4694, https://doi.org/10.1002/2014GL060457,
640 2014.
641 Gomez, B., Ewin, T. A., Daviero-Gomez, V.: The conifer *Glenrosa falcata* sp. nov. from the
642 Lower Cretaceous of Spain and its palaeoecology, Review of Palaeobotany and
643 Palynology, 172, 21–32, https://doi.org/10.1016/j.revpalbo.2012.01.009, 2012.
644 Grein, M., Oehm, C., Konrad, W., Utescher, T., Kunzmann, L., Roth-Nebelsick, A.: Atmospheric
645 CO_2 from the late Oligocene to early Miocene based on photosynthesis data and fossil
646 leaf characteristics, Palaeogeography, Palaeoclimatology, Palaeoecology, 374, 41–51,
647 https://doi.org/10.1016/j.palaeo.2012.12.025, 2013.
648 Grimaldi, D., Engel, M.S. (Eds.): Evolution of the Insects, Cambridge University Press, New York,
649 pp. 772, 2005.
650 Gröcke, D.R., Price, G.D., Robinson, S.A., Baraboshkin, E.Y., Mutterlose, J., Ruffell, A.H.: The
651 Upper Valanginian (Early Cretaceous) positive carbon–isotope event recorded in
652 terrestrial plants, Earth Planet. Sci. Lett., 240, 495–509,
653 https://doi.org/10.1016/j.epsl.2005.09.001, 2005.
654 Hansen, K.W., Wallmann, K.: Cretaceous and Cenozoic evolution of seawater composition,
655 atmospheric O_2 and CO_2, American Journal of Science, 303,
656 https://doi.org/10.2475/ajs.303.2.94, 2003.
657 Harris, T.M.: Naming a fossil conifer, J. Sen. Memorial, 243–252, 1969.
658 Haworth ,M., Heath, J., Mcelwain, J.C.: Differences in the response sensitivity of stomatal index
659 to atmospheric CO_2 among four genera of Cupressaceae conifers, Annals of Botany, 105,
660 411–418, https://doi.org/10.1093/aob/mcp309, 2010.
661 Haworth, M., Hesselbo, S.P., Mcelwain, J.C., Robinson, S.A., Brunt, J.W.: Mid-Cretaceous pCO_2
662 based on stomata of the extinct conifer *Pseudofrenelopsis* (Cheirolepidiaceae), Geology,
663 33, 749–752, https://doi.org/10.1130/G21736.1, 2005.
664 Heimhofer, U., Hochulib, P.A., Herrlec, J.O., Andersend, N., Weisserta, H.: Absence of major
665 vegetation and palaeoatmospheric pCO_2 changes associated with oceanic anoxic event 1a
666 (Early Aptian, SE France), Earth Planet. Sci. Lett., 223, 303–318,

https://doi.org/10.5194/cp-2021-96
Preprint. Discussion started: 24 August 2021

https://doi.org/10.1016/j.epsl.2004.04.037, 2004.

Huang, C.M., Retallack, G.J., Wang, C.S.: Early Cretaceous atmospheric pCO_2 levels recorded from pedogenic carbonates in China, Cretaceous Research, 33, 42–49, https://doi.org/10.1016/j.cretres.2011.08.001, 2012.

Huo, T.F., Yang D.B., Xu, W.L., Wang F., Liu H.B., Shi J.P.: U-Pb Ages and Hf Isotope Compositions of Detrital Zircons from the Sandstone in the Early Cretaceous Wawukuang Formation in the Jiaolai Basin, Shandong Province and its Tectonic Implications, Geotectonica et Metallogenia, 39(2), 355–368, 2015.

Jelby, M.E., Śliwińska, K.K., Koevoets, M.J., Alsen, P., Vickers, M.L., Olaussen, S., Stemmerik, L.: Arctic reappraisal of global carbon-cycle dynamics across the Jurassic–Cretaceous boundary and Valanginian Weissert Event, Palaeogeography, Palaeoclimatology, Palaeoecology, 555, 109847, https://doi.org/10.1016/j.palaeo.2020.109847, 2020.

Jenkyns, H.C.: Geochemistry of Oceanic Anoxic Events, Geochemistry, Geophysics, Geosystems, 11(3), Q03004, doi:10.1029/2009GC002788, 2010.

Jin, P.H., Dong, J.L., Wang, Z.X., Yuan, X.C., Hua, Y.F., Du, B.X., Sun, B.N.: A new species of *Elatides* from the Lower Cretaceous in Shandong province, Eastern China and its geographic significance, Cretaceous Research, 85, 109–127, https://doi.org/10.1016/j.cretres.2017.11.022, 2018.

Jin, P.H., Mao, T., Dong, J.L., Wang, Z.X., Xu, X,H., Du, B.X., Sun, B.N.: A new species of *Cupressinocladus* from the Lower Cretaceous of Guyang Basin, Inner Mongolia, North China and its microstructure, Acta Geological Sinica (English Edition), 4, 1200–1214, https://doi.org/10.1111/1755-6724.13355, 2017.

Kemper, E., Schmitz, H.H.: Glendonite-Indikatoren des polarmarinen Ablagerungsmilieus, Geol. Rundsch., 2, 759–773, 1981.

Konrad, W., Katul, G., Roth-Nebelsick, A., Grein, M.: A reduced order model to analytically infer atmospheric CO_2 concentration from stomatal and climate data, Advances in Water Resources, 104, 145–157, https://doi.org/10.1016/j.advwatres.2017.03.018, 2017.

Konrad, W., Roth–Nebelsick, A., Grein, M.: Modelling of stomatal density response to atmospheric CO_2, Journal of Theoretical Biology, 253(4), 638–658, https://doi.org/10.1016/j.jtbi.2008.03.032, 2008.

Kürschner, W.M., Kvaček, Z., Dilcher, D.L.: The impact of Miocene atmospheric carbon dioxide fluctuations on climate and the evolution of terrestrial ecosystems, Proceedings of the National Academy of Sciences, 105, 449–453, https://doi.org/10.1073/pnas.0708588105, 2008.

Lee, Y.I.: Stable isotopic composition of calcic paleosol of the Early Cretaceous Hasandong Formation, southeastern Korea, Palaeogeography, Palaeoclimatology, Palaeoecology, 150 (1–2), 123–133, https://doi.org/10.1016/S0031-0182(99)00010-3, 1999.

Lee, Y.I., Hisada, K.I.: Stable isotopic composition of pedogenic carbonates of the Early Cretaceous Shimonoseki Subgroup, western Honshu, Japan, Palaeogeography, Palaeoclimatology, Palaeoecology, 153 (1–4), 127–138, https://doi.org/10.1016/S0031-0182(99)00069-3, 1999.

Lei, X.T.: Early Cretaceous Cheirolepidiaceae from the Jiuquan and Liupanshan Basins and pCO_2 estimates, Ph.D. thesis, Lanzhou University, China, 27–40pp., 2019 (in Chinese with English abstract).

https://doi.org/10.5194/cp-2021-96
Preprint. Discussion started: 24 August 2021

711 Lei, X.T., Du, Z., Du, B.X., Zhang, M.Z., Sun, B.N.: Middle Cretaceous pCO_2 variation in Yumen,
712 Gansu Province and its response to the climate events, Acta Geologica Sinica-English
713 Edition, 92(2), 801–813, https://doi.org/10.1111/1755-6724.13555, 2018.
714 Leier, Heimhofer A., Quade, J., DeCelles, P., Kapp, P.: Stable isotopic results from paleosol
715 carbonate in South Asia: paleoenvironmental reconstructions and selective alteration,
716 Earth Planet. Sci. Lett., 279, 242–254, https://doi.org/10.1016/j.epsl.2008.12.044, 2009.
717 Li, H., Yu, J.X., McElwain, J.C., Yiotis, C., Chen, Z.Q.: Reconstruction of atmospheric CO_2
718 concentration during the late Changhsingian based on fossil conifers from the Dalong
719 Formation in South China, Palaeogeography, Palaeoclimatology, Palaeoecology, 519, 37–
720 48, https://doi.org/10.1016/j.palaeo.2018.09.006, 2019.
721 Li, R.H., Zhang, G.W.: New Dinosaur Ichotaxon from the Early Cretaceous Laiyang Group in the
722 Laiyang Basin, Shandong Province, Geological review, 46(6), 605–610, 2000 (in Chinese
723 with English abstract).
724 Lin, Q.: On Penaphis Lin, 1980 of Cretaceous (Callaphididae, Homoptera) and its coevolutionary
725 relationships, Acta Palaeontologica Sinica, 34, 194–204, 1995 (in Chinese with English
726 abstract).
727 Ling, W.L., Xie, X.J., Liu, X.M., Cheng, J.P.: Zircon U-Pb dating on the Mesozoic volcanic suite
728 from the Qingshan Group stratotype section in eastern Shandong Province and its tectonic
729 significance, Science in China, 50(6), 813–824, 2007.
730 Lini, A., Weissert, H., Erba, E.: The Valanginian carbon isotope event: a first episode of
731 greenhouse climate conditions during the Cretaceous, Terra Nova, 4, 374–384,
732 https://doi.org/10.1111/j.1365-3121.1992.tb00826.x, 1992.
733 Luo, S.L., Liu, M.W., Sha, Y.X., Wang, B., Hong, Y.C., Wang, W.L., Yu, J.X. (Eds.): The
734 stratigraphy and palaeontology of Laiyang Basin, Shandong province, Geological
735 Publishing House, Beijing pp. 24–159, 1990.
736 Martinez, M., Deconinck, J.F., Pellenard, P., Riquier, L., Company, M., Reboulet, S., Moiroud, M.:
737 Astrochronology of the Valanginian–Hauterivian stages (Early Cretaceous):
738 Chronological relationships between the Paraná–Etendeka large igneous province and
739 the Weissert and the Faraoni events, Global and Planetary Change, 131, 158–173,
740 https://doi.org/10.1016/j.gloplacha.2015.06.001, 2015.
741 McArthur, J.M., Janssen, N.M.M., Reboulet, S., Leng, M.J., Thirlwall, M.F., van de Schootbrugge,
742 B.: Palaeotemperatures, polar ice-volume, and isotope stratigraphy (Mg/Ca, $\delta^{18}O$, $\delta^{13}C$,
743 $^{87}Sr/^{86}Sr$): the Early Cretaceous (Berriasian, Valanginian, Hauterivian),
744 Palaeogeography, Palaeoclimatology, Palaeoecology, 248, 391–430,
745 https://doi.org/10.1016/j.palaeo.2006.12.015, 2007.
746 Mcelwain, J.C.: Do fossil plants signal palaeoatmospheric carbon dioxide concentration in the
747 geological past? Philosophical Transactions Biological Sciences, 353, 83–96,
748 https://doi.org/10.1098/rstb.1998.0193, 1998.
749 McElwain, J.C., Chaloner, W.G.: Stomatal density and index of fossil plants track atmospheric
750 carbon dioxide in the Palaeozoic, Annals of Botany, 76, 389–395,
751 https://doi.org/10.1006/anbo.1995.1112, 1995.
752 Mcelwain, J.C., Chaloner, W.G.: The Fossil Cuticle as a Skeletal Record of Environmental
753 Change, Palaios, 11, 376–388, https://doi.org/10.2307/3515247, 1996.
754 Meissner, P., Mutterlose, J., Bodin, S.: Latitudinal temperature trends in the northern hemisphere

https://doi.org/10.5194/cp-2021-96
Preprint. Discussion started: 24 August 2021

during the Early Cretaceous (Valanginian–Hauterivian), Palaeogeography, Palaeoclimatology, Palaeoecology, 424, 17–39, https://doi.org/10.1016/j.palaeo.2015.02.003, 2015.

Miller, C.N.: Mesozoic conifers, The Botanical Review, 43(2), 217–280, 1977.

Möller, C., Bornemann A., Mutterlose J.: Climate and paleoceanography controlled size variations of calcareous nannofossils during the Valanginian Weissert Event (Early Cretaceous), Marine Micropaleontology, 157, 101875, https://doi.org/10.1016/j.marmicro.2020.101875, 2020.

OKUBO, A., KIMURA, T.: *Cupressinocladus obatae*, sp. nov., from the Lower Cretaceous Choshi Group, in the Outer Zone of Japan, Bulletin of the National Science Museum, Series C, 17(3), 91–109, 1991.

O'Reilly, J.E., Reis, M. dos, Donoghue, P.C.J.: Dating tips for divergence-time estimation, Trends in Genetics, 31 (11), 637–650, https://doi.org/10.1016/j.tig.2015.08.001, 2015.

Passalia, M.G.: Cretaceous pCO_2 estimation from stomatal frequency analysis of gymnosperm leaves of Patagonia, Argentina, Palaeogeography, Palaeoclimatology, Palaeoecology, 273, 17–24, https://doi.org/10.1016/j.palaeo.2008.11.010, 2009.

Pearson, P.N., Palmer, M.R.: Atmospheric carbon dioxide concentrations over the past 60 million years, Nature, 406, 695, 2000.

Podlaha, O.G., Mutterlose, J., Veizer, J.: Preservation of $\delta^{18}O$ and $\delta^{13}C$ in belemnite rostra from the Jurassic/ Early Cretaceous successions, American Journal of Science, 324–347, https://doi.org/10.2475/ajs.298.4.324, 1998.

Price, G.D., Janssen, N.M.M., Martinez, M., Company, M., Vandevelde, J.H., Grimes, S.T.: A high-resolution belemnite geochemical analysis of Early Cretaceous (Valanginian-Hauterivian) environmental and climatic perturbations, Geochemistry, Geophysics, Geosystems, 19, 3832–3843, https://doi.org/10.1029/2018GC007676, 2018.

Price, G.D., Mutterlose, J.: Isotopic signals from late Jurassic–early Cretaceous (Volgian–Valanginian) sub-Arctic belemnites, Yatria River, Western Siberia, J. Geol. Soc., 161, 959–968, https://doi.org/10.1144/0016-764903-169, 2004.

Quan, C., Sun, C., Sun, Y., Sun, G.: High resolution estimates of paleo-CO_2 levels through the Campanian (Late Cretaceous) based on Ginkgo cuticles, Cretaceous Research, 30, 424–428, https://doi.org/10.1016/j.cretres.2008.08.004, 2009.

Reichgelt, T., D'Andrea, W.J.: Plant carbon assimilation rates in atmospheric CO_2 reconstructions, New Phytologist, 223, 1844–1855, https://doi.org/10.1111/nph.15914, 2019.

Ren, D., Hong, Y.: Origin of angiosperms based on the flower-loving Brachycera fossils, Acta Zootaxonomica Sinica, 23, 212–221, 1998 (in Chinese with English abstract).

Retallack, G.J.: A 300–million–year record of atmospheric carbon dioxide from fossil plant cuticles, Nature, 411, 287, 2001.

Retallack, G.J.: Pedogenic carbonate proxies for amount and seasonality of precipitation in paleosols, Geology, 33, 333–336, https://doi.org/10.1130/G21263.1, 2005.

Retallack, G.J.: Refining a pedogenic-carbonate CO_2 paleobarometer to quantify a middle Miocene greenhouse spike, Palaeogeography, Palaeoclimatology, Palaeoecology, 281(1–2), 57–65, https://doi.org/10.1016/j.palaeo.2009.07.011, 2009a.

Retallack, G.J.: Greenhouse crises of the past 300 million years, Geological Society of America Bulletin, 121, 1441–1455, https://doi.org/10.1130/B26341.1, 2009b.

https://doi.org/10.5194/cp-2021-96
Preprint. Discussion started: 24 August 2021

799 Robinson, S.A., Andrews, J.E., Hesselbo, S.P., Radley, J.D., Dennis, P.F., Harding, I.C., Allen, P.:
800 Atmospheric pCO_2 and depositional environment from stable-isotope geochemistry of
801 calcrete nodules (Barremian, Lower Cretaceous, Wealden Beds, England), J. Geol. Soc.,
802 159, 215–224, https://doi.org/10.1144/0016-764901-015, 2002.
803 Royer, D.L.: CO_2-forced climate thresholds during the Phanerozoic, Geochim. Cosmochim. Acta,
804 70, 5665–5675, https://doi.org/10.1016/j.gca.2005.11.031, 2006.
805 Royer, D.L., Moynihan, K.M., McKee, M.L., Londoño, L., Franks, P.J.: Sensitivity of a leaf gas-
806 exchange model for estimating paleoatmospheric CO_2 concentration, Climate of the Past,
807 15, 795–809, https://doi.org/10.5194/cp-15-795-2019, 2019.
808 Schubert, B.A., Jahren, A.H.: The effect of atmospheric CO_2 concentration on carbon isotope
809 fractionation in C_3 land plants, Geochim. Cosmochim. Acta, 96, 29–43,
810 https://doi.org/10.1016/j.gca.2012.08.003, 2012.
811 Schubert, B.A., Jahren, A.H.: Global increase in plant carbon isotope fractionation following the
812 Last Glacial Maximum caused by increase in atmospheric pCO_2, Geology, 43 (5), 435–
813 438, https://doi.org/10.1130/G36467.1, 2015.
814 Shi, G.L., Zhou, Z.Y., Xie, Z.M.; *Cupressus* foliage shoots and associated seed cones from the
815 Oligocene Ningming Formation of Guangxi, South China, Review of Palaeobotany and
816 Palynology, 166(3), 325–334, https://doi.org/10.1016/j.revpalbo.2011.06.005, 2011.
817 Skelton, P.W., Spicer, R.A., Kelley, S.P., Gilmour, I.: The Cretaceous World, 2003.
818 Srinivasan, V.: Two new species of the conifer *Glenrosa* from the Lower Cretaceous of North
819 America, Review of Palaeobotany and Palynology, 72, 245–255,
820 https://doi.org/10.1016/0034-6667(92)90029-G, 1992.
821 Srinivasan, V.: Conifers from the Puddledock locality (Potomac Group, Early Cretaceous) in
822 eastern North America, Review of Palaeobotany and Palynology, 89(3–4), 257–286,
823 https://doi.org/10.1016/0034-6667(95)00010-8, 1995.
824 Steinthorsdottir, M., Jeram, A.J., McElwain, J.C.: Extremely elevated CO_2 concentrations at the
825 Triassic/Jurassic boundary, Palaeogeography, Palaeoclimatology, Palaeoecology, 308,
826 418–432, https://doi.org/10.1016/j.palaeo.2011.05.050, 2011.
827 Steinthorsdottir, M., Vajda, V.: Early Jurassic (late Pliensbachian) CO_2 concentrations based on
828 stomatal analysis of fossil conifer leaves from eastern Australia, Gondwana Res., 27,
829 932–939, https://doi.org/10.1016/j.gr.2013.08.021, 2015.
830 Steinthorsdottir, M., Wohlfarth, B., Kylander, M.E., Blaauw, M., Reimer, P.J.: Stomatal proxy
831 record of CO_2 concentrations from the last termination suggests an important role for CO_2
832 at climate change transitions, Quat. Sci. Rev., 68, 43–58,
833 https://doi.org/10.1016/j.gr.2013.08.021, 2013.
834 Sun, B.N., Xiao, L., Xie, S.P., Deng, S.H., Wang, Y.D., Jia, H., Turner, S.: Quantitative analysis
835 of paleoatmospheric CO_2 level based on stomatal characters of fossil *Ginkgo* from
836 Jurassic to Cretaceous in China, Acta Geol. Sin., 81, 931–939,
837 https://doi.org/10.1111/j.1755-6724.2007.tb01016.x, 2007.
838 Sun, Y.W., Li, X., Zhao, G.W., Liu, H., Zhang, Y.L.: Aptian and Albian atmospheric CO_2 changes
839 during oceanic anoxic events: evidence from fossil *Ginkgo* cuticles in Jilin Province,
840 Northeast China, Cretaceous Research, 62, 130–141,
841 https://doi.org/10.1016/j.cretres.2015.12.007, 2016.
842 Tajika, E.: Carbon cycle and climate change during the Cretaceous inferred from a

https://doi.org/10.5194/cp-2021-96
Preprint. Discussion started: 24 August 2021

Climate of the Past Discussions

biogeochemical carbon cycle model, Island Arc, 8, 293–303, https://doi.org/10.1046/j.1440-1738.1999.00238.x, 1999.

Wallmann, K.: Controls on the Cretaceous and Cenozoic evolution of seawatercomposition, atmospheric CO_2 and climate, Geochim. Cosmochim. Acta, 65, 3005–3025, https://doi.org/10.1016/S0016-7037(01)00638-X, 2001.

Wan, C.B., Wang, D.H., Zhu, Z.P., Quan, C.: Trend of Santonian (Late Cretaceous) atmospheric CO_2 and global mean land surface temperature: evidence from plant fossils, Earth Sci., 54, 1338–1345, doi: 10.1007/s11430-011-4267-1, 2011.

Wang, Y.D., Huang, C.M., Sun, B.N., Quan, C., Wu, J.Y., Lin, Z.C.: Paleo-CO_2 variation trends and the Cretaceous greenhouse climate, Earth-Science Reviews, 129, 136–147, https://doi.org/10.1016/j.earscirev.2013.11.001, 2014.

Watson, J.: The Cheirolepidiaceae. In: Origin and Evolution of Gymnosperms, edited by: Beck, C.B., Columbia University Press, New York, pp. 382–447, 1988.

Watson, J., Fisher, H.L.: A new conifer genus from the Lower Cretaceous Glen Rose Formation, Texas, Palaeontology, 77, 719–727, 1984.

Weissert, H., Erba, E.: Volcanism, CO_2 and palaeoclimate: a Late Jurassic-Early Cretaceous carbon and oxygen isotope record, Journal of the Geological Society, 161, 695–702, https://doi.org/10.1144/0016-764903-087, 2004.

Wortmann, U.G., Weissert, H.: Tying platform drowning to perturbations of the global carbon cycle with a $\delta^{13}C_{Org}$-curve from the Valanginian of DSDP Site 416, Terra Nova, 12, 289–294, https://doi.org/10.1046/j.1365-3121.2000.00312.x, 2000.

Xie, S.W., Wu, Y.B., Zhang, Z.M., Qin, Y.C., Liu, X.C., Wang, H., Qin, Z.W., Liu, Q., Yang, S.H.: U-Pb ages and trace elements of detrital zircons from Early Cretaceous sedimentary rocks in the Jiaolai Basin, north margin of the Sulu UHP terrane: Provenances and tectonic implications, Lithos, 154, 346–360, https://doi.org/10.1016/j.lithos.2012.08.002, 2012.

Zhang, J.F., Rasnitsyn, A.P.: New extinct taxa of Pelecinidae sensu lato (Hymenoptera: Proctotrupoidea) in the Laiyang Formation, Shandong, China, Cretaceous Research, 27 (5), 684–688, https://doi.org/10.1016/j.cretres.2006.03.001, 2006.

Zhang, Y.Q., Dong, S.W., Shi, W.: Cretaceous deformation history of the middle Tan2Lu fault zone in Shandong Province, Eastern China, Tectonophysics, 363 (324), 243–258, https://doi.org/10.1016/S0040-1951(03)00039-8, 2003.

Zhang, Y.Q., Li, J.L., Zhang, T., Dong, S.W., Yuan, J.Y.: Cretaceous to Paleocene TectonoeSedimentary Evolution of the Jiaolai Basin and the Contiguous Areas of the Shandong Peninsula (North China) and Its Geodynamic Implications, Acta Geologica Sinica, 82 (9), 1229–1257, 2008 (in Chinese with English abstract).

Zhou, N., Wang, Y.D., Ya, L., Porter, A.S., Kürschner, W.M., Li, L.Q., Lu, N., McElwain, J.C.: An inter-comparison study of three stomatal-proxy methods for CO_2 reconstruction applied to early jurassic ginkgoales plants, Palaeogeography, Palaeoclimatology, Palaeoecology, 542(15), 109547, https://doi.org/10.1016/j.palaeo.2019.109547, 2020.